



Synthesis and biological activity of novel mono-indole and mono-benzofuran inhibitors of bacterial transcription initiation complex formation



Marcin Mielczarek^a, Ruth V. Thomas^a, Cong Ma^c, Hakan Kandemir^{a,e}, Xiao Yang^c, Mohan Bhadbhade^a, David StC. Black^a, Renate Griffith^d, Peter J. Lewis^c, Naresh Kumar^{a,b,*}

^a School of Chemistry, UNSW Australia, Sydney, NSW 2052, Australia

^b Australian Centre for Nanomedicine, University of New South Wales, Sydney 2052, Australia

^c School of Environmental and Life Sciences, University of Newcastle, Callaghan, NSW 2308, Australia

^d School of Medical Sciences, Department of Pharmacology, UNSW Australia, Sydney, NSW 2052, Australia

^e School of Chemistry, Faculty of Art and Science, Namik Kemal University, Turkey

ARTICLE INFO

Article history:

Received 9 January 2015

Revised 12 February 2015

Accepted 17 February 2015

Available online 25 February 2015

Keywords:

Mono-indoles

Mono-benzofurans

RNA polymerase

σ^{70}/σ^A factors

Antibacterial activity

Structure–activity relationship (SAR)

ABSTRACT

Our ongoing research focused on targeting transcription initiation in bacteria has resulted in synthesis of several classes of mono-indole and mono-benzofuran inhibitors that targeted the essential protein–protein interaction between RNA polymerase core and σ^{70}/σ^A factors in bacteria. In this study, the reaction of indole-2-, indole-3-, indole-7- and benzofuran-2-glyoxyloyl chlorides with amines and hydrazines afforded a variety of glyoxyloylamides and glyoxyloylhydrazides. Similarly, condensation of 2- and 7-trichloroacetylindoles with amines and hydrazines delivered amides and hydrazides. The novel molecules were found to inhibit the RNA polymerase– σ^{70}/σ^A interaction as measured by ELISA, and also inhibited the growth of both Gram-positive and Gram-negative bacteria in culture. Structure–activity relationship (SAR) studies of the mono-indole and mono-benzofuran inhibitors suggested that the hydrophilic–hydrophobic balance is an important determinant of biological activity.

© 2015 Elsevier Ltd. All rights reserved.

1. Introduction

Antibiotics have been of fundamental importance in contemporary medicine and pharmacy since the discovery of penicillin, an antibacterial agent from the fungus *Penicillium notatum* by Alexander Fleming in 1928.^{1,2} However, as a result of their excessive and sometimes unjustified use, bacterial strains resistant to these drugs have rapidly emerged.^{3–25} The loss of potency of existing antibiotics against resistant strains has been exacerbated by the continually decreasing numbers of new antimicrobial compounds being brought to the market.^{26–28}

Current antibacterial drug discovery is largely focused on the derivatization of existing classes of antibiotics. However, such compounds may be prone to inactivation by existing bacterial resistance mechanisms. Therefore, in order to combat the rise and spread of antibiotic resistant strains, the discovery and

development of novel classes of antibiotics and the elucidation of their molecular targets have to be urgently pursued.²⁹

Bacterial RNA polymerase (RNAP) is an attractive target for novel antibacterial agents. Several classes of antibiotics have been discovered that inhibit the activity of RNAP via different molecular mechanisms, and some of these molecules are important components of antibacterial therapies.^{30–39} However, only a few classes of antibacterial agents targeting bacterial transcription initiation complex formation, and in particular the β' -CH- $\sigma^{70}/\sigma^A_{2.2}$ protein–protein interaction, have been discovered.^{2,32,34,35,40} Synthetic molecules **1**, **2** and **3** have been found to efficiently inhibit transcription initiation in bacteria (Fig. 1).^{34,35}

Bacterial transcription is a sequential process comprising three main stages: initiation, elongation and termination.⁴¹ There are two forms of bacterial RNAP: core and holoenzyme.⁴¹ Both enzyme forms are catalytically active, but only the holoenzyme formed by the association of the core enzyme with σ factors is able to recognize DNA promoter sequences and initiate transcription with appropriate specificity and efficiency.^{41–48} The RNAP core enzyme consists of five subunits: α_2 dimer, β , β' and ω .^{32,41} σ factors are

* Corresponding author. Tel.: +61 2 9385 4698; fax: +61 2 9385 6141.

E-mail address: n.kumar@unsw.edu.au (N. Kumar).

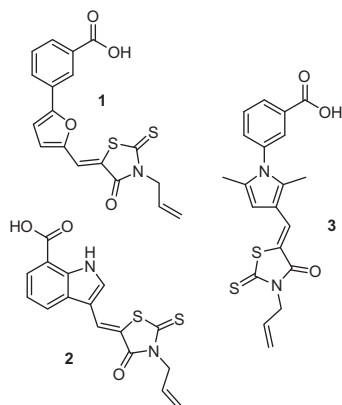


Figure 1. Synthetic molecules inhibiting transcription initiation.

unique to bacteria and the closely related σ^{70} factors in Gram-negative bacteria, and σ^A factors in Gram-positive bacteria are essential and required for the transcription of the majority of expressed genes.² The RNAP holoenzyme is formed via protein–protein interaction between two highly conserved motifs: the β' -CH region of RNAP core and region 2.2 of the σ^{70}/σ^A factor.⁴⁹ Since the regions of the σ^{70}/σ^A factor family that interact with the RNAP core enzyme are highly conserved across different bacteria species,^{32,42,44,48,50,51} molecules capable of inhibiting the β' -CH- $\sigma^{70}/\sigma_{2.2}^A$ interaction would be expected to exhibit broad spectrum antibacterial activity. Therefore, the design and development of such novel drug candidates, potentially unique both in terms of their mechanism of antibacterial activity as well as in the structure of their chemical scaffolds, could help to combat bacterial infections that are resistant to currently used antibiotics.

Our previous research aimed at the identification of potential inhibitors of the β' -CH- $\sigma^{70}/\sigma_{2.2}^A$ protein–protein interaction resulted in the synthesis of a library of novel bis-indole compounds capable of efficiently disrupting this interaction in a cell-free assay.² Modelling studies based on a *Bacillus subtilis* RNAP homology model⁵² and isothermal titration calorimetry experiments⁴⁰ proved that the bis-indoles inhibited transcription initiation by binding to the β' -CH region of the RNAP core enzyme. Interestingly, many of the synthesized molecules were found to exclusively inhibit the growth of *Escherichia coli*,² allowing them to potentially be used as non-conventional antibacterial agents against Gram-negative bacteria.^{53–55} Compounds **4** and **5** were the most potent inhibitors of *E. coli* and *B. subtilis* growth, respectively (Fig. 2).²

Since the bis-indoles synthesized in our previous studies were relatively large, issues related to solubility as well as limited

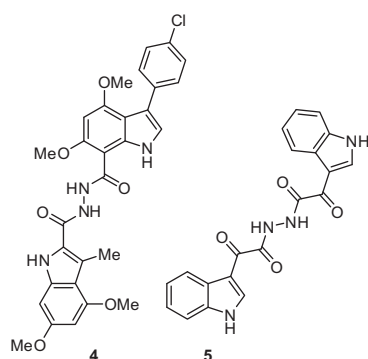


Figure 2. Bis-indole inhibitors of the interaction between RNAP core and σ^{70}/σ^A in bacteria.

penetration through the outer membrane in Gram-negative bacteria or the cell wall in Gram-positive bacteria were encountered.² Given that the indole nucleus has been discovered to be a bioactive moiety against bacterial transcription initiation complex formation, we were interested in developing smaller compounds based on indole or the related benzofuran scaffolds that could circumvent the problems associated with the larger bis-indoles, while retaining potent antibacterial activity.

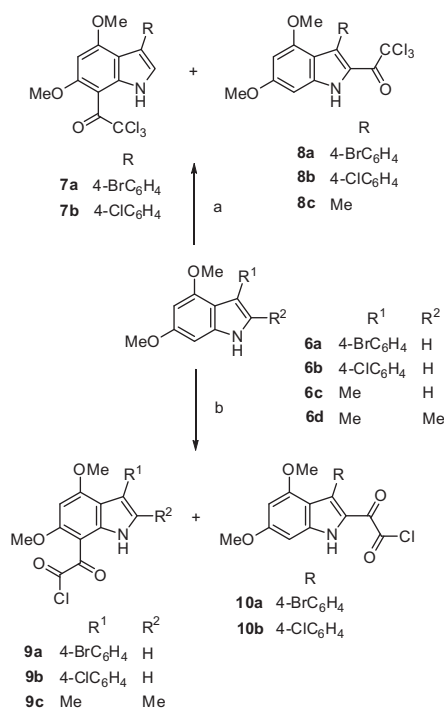
In this paper, we report the synthesis and evaluation of the antibacterial activity of a library of low molecular weight molecules active against both Gram-positive and Gram-negative bacteria, and present our structure–activity relationship (SAR) studies on these novel inhibitors of the essential β' -CH- $\sigma^{70}/\sigma_{2.2}^A$ protein–protein interaction.

2. Results and discussion

2.1. Synthesis of starting materials

In order to produce a library of mono-indole- and mono-benzofuran-based amides, hydrazides, glyoxyloylamides and glyoxyloylhydrazides, we employed well-established procedures that had previously been developed in our group for the synthesis of the biologically active bis-indoles **4** and **5** (Fig. 2).² 3-Aryl-4,6-dimethoxyindoles **6a–b**,⁵⁶ 4,6-dimethoxy-3-methylindole **6c**⁵⁶ and 4,6-dimethoxy-2,3-dimethylindole **6d**⁵⁷ were synthesized according to previously reported methods. These indoles were subsequently reacted with trichloroacetyl chloride and oxalyl chloride to yield a variety of derivatives, including 7-trichloroacetylindoles **7a–b**, 2-trichloroacetylindoles **8a–c**, indole-7-glyoxyloyl chlorides **9a–b** and indole-2-glyoxyloyl chlorides **10a–b** (Scheme 1).²

Following another well-established method developed by our group, 4,6-dimethoxy-3-phenylbenzofuran **11**⁵⁸ was synthesized and subsequently reacted with oxalyl chloride to afford benzofuran-2-glyoxyloyl chloride **12**. Additionally, indole **13** was treated



Scheme 1. Reagents and conditions: (a) CCl₃COCl (3 equiv), anhydrous 1,2-dichloroethane, 80 °C, 3.5 h, 20–37% (**7a–b**), 10–23% (**8a–c**); (b) oxalyl chloride (3 equiv), anhydrous diethyl ether, 0 °C → rt, 3 h, 30–33% (**9a–b**), 35–43% (**10a–b**).

with oxalyl chloride, yielding indole-3-glyoxyloyl chloride **14**⁵⁹ (Scheme 2).

2.2. Synthesis of glyoxyloylamides and glyoxyloylhydrazides

When indole-2-glyoxyloyl chlorides **10a–b**, indole-3-glyoxyloyl chloride **14** and benzofuran-2-glyoxyloyl chloride **12** were reacted with a variety of excess amines, the corresponding indole-2-glyoxyloylamides **15a–l**, indole-3-glyoxyloylamides **17a–d** and benzofuran-2-glyoxyloylamides **18a–d**, respectively, were synthesized in 10–55% yield (Fig. 3).

The range of amines used included secondary heterocyclic amines such as piperidine, morpholine, pyrrolidine, *N*-methyl-piperazine, *N*-benzylpiperazine and *N*-(pyridin-2-yl)piperazine, and primary aliphatic amines such as ethyl glycinate. The reactions were carried out in anhydrous diethyl ether at room temperature for 3–6 h or in anhydrous 1,2-dichloroethane at 60–70 °C for 3 h. Indole-3-glyoxyloylamides **17a–b** have been previously reported.⁶⁰

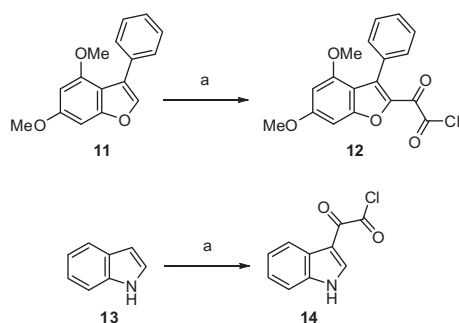
In a similar manner, indole-7-glyoxyloylamides **16a–m** and indole-7-glyoxyloylhydrazides **16n–o** were produced in 27–88% yield when the indole-7-glyoxyloyl chlorides **9a–c** were treated with excess secondary heterocyclic amines, primary aromatic amines such as aniline and *p*-toluidine, or phenylhydrazine in anhydrous diethyl ether at room temperature for 1–6 h (Fig. 3). An ORTEP diagram⁶¹ showing one of the four independent molecules for **16a** is presented in Figure 4.

2.3. Synthesis of carboxamides and carboxhydrazides

The indole-2-carboxamide **19** was synthesized in 69% yield from the reaction between 2-trichloroacetylindole **8b** and morpholine in anhydrous acetonitrile at room temperature for 9 h (Fig. 5). Similarly, the reaction of 7-trichloroacetylindoles **7a–b** with aniline and *p*-toluidine in anhydrous acetonitrile at reflux for 12 h afforded the respective indole-7-carboxamides **20a–c** in 51–60% yield. Reactions of 7-trichloroacetylindoles **7a–b** and phenylhydrazine in anhydrous acetonitrile at room temperature for 3 h resulted in formation of indole-7-carboxhydrazides **20d–e** in 61% yield (Fig. 5).

2.4. Evaluation of biological activity

The library of thirty-nine synthesized compounds was then evaluated for antibacterial activity. The inhibition of the interaction between $\sigma^{70}/\sigma_{2.2}^A$ and the β' -CH region of the core RNAP was examined by ELISA at 15 μ M concentration of compound and is expressed as a % inhibition of the negative control (the interaction between $\sigma^{70}/\sigma_{2.2}^A$ and β' -CH in the absence of the inhibitor). Bacterial growth



Scheme 2. Reagents and conditions: (a) oxalyl chloride (3 equiv), anhydrous diethyl ether, 0 °C → rt, 3 h, 92% (**14**).

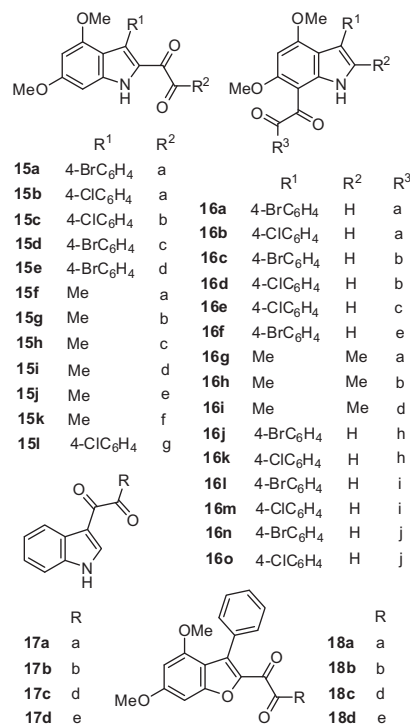


Figure 3. Glyoxyloylamides and glyoxyloylhydrazides; a = piperidin-1-yl, b = morpholin-1-yl, c = pyrrolidin-1-yl, d = *N*-(pyridin-2-yl)piperazin-1-yl, e = *N*-benzylpiperazin-1-yl, f = *N*-methylpiperazin-1-yl, g = ethyl 2-aminoacetyl, h = anilinyll, i = toluidinyl, j = phenylhydrazinyl.

inhibition was evaluated at ca. 200 μ M compound concentration using two representative bacterial species, *B. subtilis* (Gram-positive) and *E. coli* (Gram-negative), and is expressed as a% inhibition of the negative control (bacterial growth in the absence of the inhibitor). Some of the molecules precipitated out of the solution when diluted to ca. 200 μ M concentration with the growth medium (Table 1).

Molecules **15l**, **16c**, **16l–m**, **16o** and **20d–e** showed significant ($\geq 20\%$) and exclusive inhibition of *E. coli* growth, with compounds **15l** and **16c** being the most potent selective inhibitors of *E. coli* growth (53% and 59% inhibition, respectively). On the other hand, molecule **16j** showed 36% inhibition of *B. subtilis* growth and 33% inhibition of *E. coli* growth, indicating its potential as a broad spectrum antibacterial agent. Compounds **15c**, **16g–h** and **18b** affected the exponential phase of *B. subtilis* growth, while molecules **16c–d** inhibited the exponential phase of *E. coli* growth.

For compounds **16c** and **18b** further experiments were performed to demonstrate concentration–response behaviour. ELISA experiments in the concentration range 2–500 μ M allowed determination of IC₅₀ values for these two compounds (33.9 \pm 3.9 μ M for **16c** and 71.6 \pm 3.0 μ M for **18b**). Inhibition of bacterial growth was also tested for these two compounds at concentrations of 13–1600 μ M (growth curves shown in Supplementary material). **16c** inhibited *E. coli* growth at concentrations of >100 μ M. Similarly, for **18b**, inhibition of *B. subtilis* growth was observed at concentrations of >100 μ M.

Molecules **16e**, **17d** and **18b** were the most potent inhibitors of *B. subtilis* growth, with growth inhibition values of 60%, 70% and 70% at 200 μ M, respectively. However, since these compounds exhibited relatively low or no activity in the ELISA, their mechanism of antibacterial activity might not involve the inhibition of the β' -CH- $\sigma^{70}/\sigma_{2.2}^A$ interaction. The same applies, but to a smaller extent, to molecules **16d**, **16e** and **19** with respect to inhibition of *E. coli* growth.

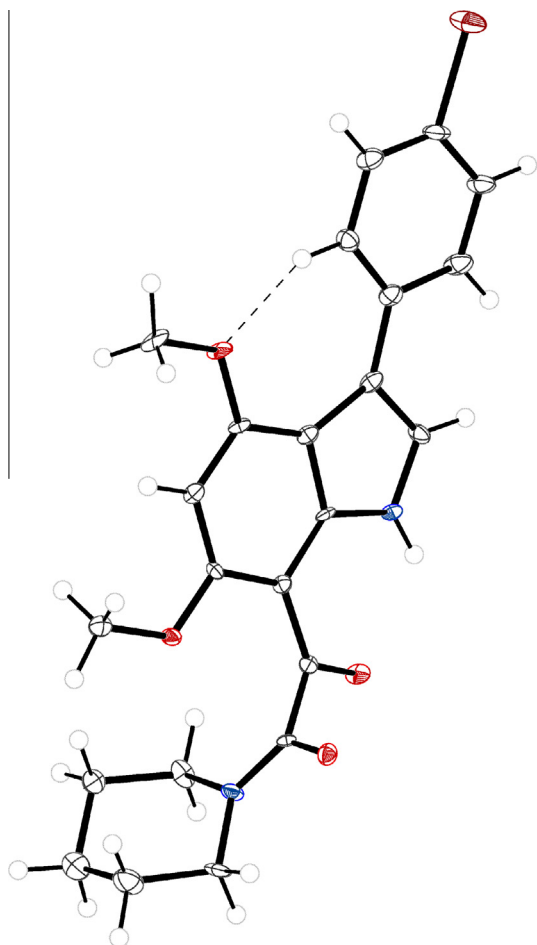


Figure 4. An ORTEP diagram showing one of the four independent molecules for **16a** (thermal ellipsoids are drawn at 50% probability level).

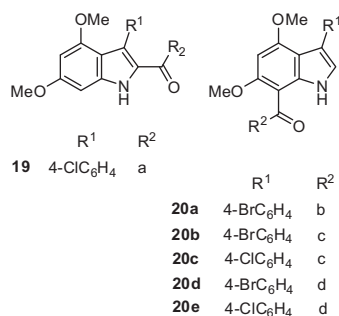


Figure 5. Amides and hydrazides; a = morpholin-1-yl, b = aniliny, c = toluidiny, d = phenylhydraziny.

2.5. Structure–activity relationship (SAR) studies

The ability of the compounds to inhibit the β' -CH- $\sigma^{70}/\sigma_{2,2}^A$ interaction can be predicted by mapping the compounds onto a pharmacophore developed earlier.⁴⁰ This pharmacophore describes the interactions the σ factor forms with the β' -CH region and was developed based on the *B. subtilis* RNAP homology model and mutagenesis experiments. Compounds which fit this pharmacophore well, mapping all features, have >80% chance of activity (>20% inhibition at 15 μM) in the ELISA assay.

The ability of the compounds to cross the cell walls of Gram-positive bacteria and the outer membranes of Gram-

Table 1
 β' -CH- $\sigma^{70}/\sigma_{2,2}^A$ binding inhibitory activity and anti-bacterial activity of the synthesized compounds.

Compound	β' -CH- $\sigma^{70}/\sigma_{2,2}^A$ binding inhibition at 15 μM by ELISA (%)	Growth inhibition at 200 μM (%)	
		<i>Bacillus subtilis</i>	<i>Escherichia coli</i>
15a	39	22 ^a	7 ^a
15b	NA	NA	18
15c	27	37 ^{a, b}	37 ^a
15d	NA	NA	NA
15e	25	19	38
15f	17	NA	NA
15g	33	2	2
15h	44	NA	NA
15i	48	14	38
15j	46	7	16
15k	44	NA	NA
15l	42	NA ^a	53 ^a
16a	32	14	26
16b	NA	NA	NA
16c	31	NA	59 ^b
16d	NA	NA	38 ^b
16e	NA	60 ^f	23
16f	8	NA	6
16g	39	57 ^b	24
16h	7	42 ^b	NA
16i	27	12	13
16j	34	36	33
16k	23	26	23
16l	ND	NA	29
16m	37	NA	20
16n	34	10 ^a	24 ^a
16o	26	NA ^a	20 ^a
17a	37	12	9
17b	39	NA	4
17c	27	10	4
17d	21	70	6
18b	29	70 ^b	6
18c	41	3	10
19	NA	NA	42
20a	49	7	13
20b	ND	36	12
20c	ND	13	13
20d	44	NA	23
20e	60	NA	21

^a Precipitation at ca. 200 μM .

^b Affects exponential phase of bacterial growth.

^c *Staphylococcus aureus*, NA: no activity, ND: not determined.

negative bacteria might account for the differences between the inhibition of the β' -CH- $\sigma^{70}/\sigma_{2,2}^A$ interaction and the inhibition of bacterial growth observed for some molecules. For example, compounds **15f–k** containing a Me substituent at position 3 of the indole ring inhibited the β' -CH- $\sigma^{70}/\sigma_{2,2}^A$ interaction with potency comparable to their structural analogues containing a C₆H₅, 4-BrC₆H₄ or 4-ClC₆H₄ substituent at the same position, but showed a dramatic decrease or even a complete loss of bacterial growth inhibitory activity. However, compound **15i** having a *N*-(pyridin-2-yl)piperazin-1-yl substituent and compound **15j** having a *N*-benzylpiperazin-1-yl substituent in a side chain at position 2 of the indole ring still exhibited low or moderate ability to inhibit bacterial growth. We hypothesize that the analogues **15i–j** containing relatively bulky and lipophilic substituents had superior ability to cross the outer membrane of Gram-negative bacteria and the cell wall of Gram-positive bacteria compared to analogues containing smaller and less lipophilic substituents, such as a piperidin-1-yl (**15f**), morpholin-1-yl (**15g**), pyrrolidin-1-yl (**15h**) and *N*-methylpiperazin-1-yl (**15k**). In compounds **15i–j**, the decrease in molecular lipophilicity resulting from replacement of an aryl substituent at position 3 of the indole ring by the smaller Me substituent is compensated by incorporation of bulky and lipophilic substituents in a side chain at position 2 of the indole

ring. This hypothesis is further strengthened by calculating $clogP$ values for these compounds in the uncharged state, with **15i–j** exhibiting the highest values (3.2 and 3.7) in the series.

In general, it was observed that an optimal $clogP$ range exists for growth inhibition of *E. coli*. For $clogP$ values below 3 no significant activity is observed and most activity is observed in the $clogP$ range of 3–4, although some compounds with high $clogP$ values show >25% growth inhibition (**15e**, **16a**, **16j**, **16l**). This is consistent with the hypothesis that the compounds cross into *E. coli* by passive transport through the outer membranes, with the reason for the upper limit of $clogP$ related to a lack of aqueous solubility. This was observed experimentally for **15a**, **15c**, **15l**, **16n**, and **16o**. Judging by the predicted solubilities, this could have affected the growth inhibitory activities of a further 24 of the tested compounds, which all had low to very low predicted solubilities (for the neutral form).

Some compounds can be protonated to a noticeable extent at piperazine 'non-amide' nitrogen with predicted pK_a values of 5.6 or higher given in square brackets (**15e** [5.6], **15i** [5.6], **15j** [7.5], **15k** [9.8], **16f** [8.1], **16i** [5.6], **17c** [5.6], **17d** [8.1], **18c** [5.6], **18d** [8.1]). This obviously improves solubility, however, the charged forms are expected to have limited ability to cross bacterial membranes.

Interestingly, compounds in general show lower activity against *B. subtilis*, and no optimal $clogP$ range was observed. Calculated $logP$, pK_a and aqueous solubility values for all the molecules are presented in Supplementary material.

The glyoxyloylamides **16a**, **16c**, **16j** and **16l**, and the glyoxyloylhydrazide **16n** bearing the larger but less electron-withdrawing 4- BrC_6H_4 substituent at position 3 of the indole ring were found to possess greater potency against both the β' -CH- $\sigma^{70}/\sigma_{2,2}^A$ interaction and bacterial growth compared to the corresponding analogues **16b**, **16d**, **16k**, **16m** and **16o** that possess the smaller but more electron-withdrawing 4- ClC_6H_4 substituent at the same position.

Since a 4- BrC_6H_4 substituent is more bulky than a 4- ClC_6H_4 substituent, its incorporation into a compound results in an increase in overall lipophilicity, as confirmed by the $clogP$ values, that might enhance the ability of the molecule in crossing the outer membrane of Gram-negative bacteria and the cell wall of Gram-positive bacteria. Therefore, the increased bacterial growth inhibition of the analogues bearing the 4- BrC_6H_4 substituent might be a result of not only an increased ability of the molecules to inhibit the β' -CH- $\sigma^{70}/\sigma_{2,2}^A$ interaction, but also an increased cellular permeability resulting in higher intracellular compound concentration for interrupting the β' -CH- $\sigma^{70}/\sigma_{2,2}^A$ interaction within cells.

Interestingly, this trend was the reverse of that observed for the previously reported bis-indole inhibitors, where the replacement of a 4- ClC_6H_4 substituent by a 4- BrC_6H_4 substituent resulted in decreased inhibition of the β' -CH- $\sigma^{70}/\sigma_{2,2}^A$ interaction and reduced bacterial growth inhibitory activity.²

One possible explanation for this might be that the bis-indole inhibitors, being relatively large, had more difficulties in crossing the outer membrane or cell wall of bacterial cells. Therefore, replacement of the 4- BrC_6H_4 substituent by the less bulky 4- ClC_6H_4 substituent in the bis-indoles might have enhanced their cellular permeability as a result of a reduction in molecular size, thereby increasing their biological activity.

3. Conclusions

A library of forty-one mono-indole- and mono-benzofuran-based glyoxyloylamides, glyoxyloylhydrazides, carboxamides and carboxhydrazides was synthesized, fully characterized and screened for its potential ability to inhibit transcription initiation

complex formation in bacteria. Inhibition of the interaction between the β' -CH region of the core RNAP and $\sigma^{70}/\sigma_{2,2}^A$ was evaluated in a cell-free system by ELISA. The compounds were also examined as potential inhibitors of *B. subtilis* and *E. coli* growth in culture.

Compared with the previously reported bis-indoles that generally exhibited high inhibition of the β' -CH- $\sigma^{70}/\sigma_{2,2}^A$ interaction,² the mono-indoles and mono-benzofurans synthesized in this work showed less potent activity. On one hand, the smaller mono-indoles and mono-benzofurans might have better cellular permeability than the larger bis-indoles, but on the other hand, the larger molecules might fit better into the binding site at the β' -CH- $\sigma^{70}/\sigma_{2,2}^A$ interface. However, the decrease in the ability of the monomeric compounds to inhibit the formation of transcription initiation assembly did not result in a significant decrease in their antibacterial ability, as evidenced by the fact that the mono-indoles and mono-benzofurans were able to inhibit bacterial growth with potency comparable to the bis-indoles. On the other hand, in contrast to the bis-indoles which preferentially inhibited *E. coli* growth,² many of the monomeric molecules were found to inhibit the growth of both *B. subtilis* and *E. coli*. Six compounds were found to be exclusive inhibitors of *E. coli* growth, while only one compound **16h** inhibited *B. subtilis* growth exclusively. This observation indicates that the mono-indole scaffolds could potentially be developed as either broad spectrum antibacterial agents, or as selective inhibitors against Gram-negative bacteria. The ability to inhibit Gram-negative bacteria is especially significant in light of the rapid emergence of resistance in Gram-negative strains such as *E. coli*, *Klebsiella pneumoniae*, *Salmonella* spp., *Proteus mirabilis* and *Pseudomonas aeruginosa* to currently used antibiotics.^{53–55}

Structure–activity relationship studies carried out on the library of mono-indole compounds suggested that both molecular size and hydrophilicity–lipophilicity balance have to be considered when designing antibacterial agents, in order to generate compounds capable of crossing the outer membrane in Gram-negative bacteria and the cell wall in Gram-positive bacteria whilst retaining appropriately high solubility.

When compared to the bis-indoles synthesized in the previous work, the monomeric compounds developed in the present study showed not only an enhancement of solubility, but also retention of significant antibacterial activity in terms of both inhibition of the β' -CH- $\sigma^{70}/\sigma_{2,2}^A$ interaction and reduction of bacterial growth in culture. Therefore, future research will be aimed at the design and synthesis of monomeric inhibitors of bacterial transcription initiation complex formation.

4. Experimental

4.1. Materials and measurement methods

Trichloroacetyl chloride was synthesized from trichloroacetic acid according to a slightly modified literature procedure.⁶² All other reagents and solvents were purchased from Ajax Finechem, Alfa Aesar, Chem-Supply and Sigma–Aldrich. No further purification was performed for commercial chemicals. Anhydrous acetonitrile and anhydrous diethyl ether were obtained from a PureSolv MD Solvent Purification System available in the School of Chemistry at UNSW. ¹H NMR and ¹³C NMR spectra were recorded in CDCl₃ and DMSO-*d*₆ on a Bruker Avance III 300 MHz spectrometer in the Nuclear Magnetic Resonance Facility in the Mark Wainwright Analytical Centre at UNSW and internally calibrated to the solvent peaks. Chemical shifts (δ) were given in parts per million (ppm). Splitting patterns were reported as a singlet (s), broad singlet (br s), doublet (d) and multiplet (m), and the observed coupling constants (*J*) provided in Hertz (Hz). Peaks were assigned where possible. Infrared spectra were acquired on a Thermo Nicolet

Avatar 370 FT-IR spectrophotometer using KBr discs. The wavenumbers (ν_{\max}) related to the transmittance minima were reported in cm^{-1} . Ultraviolet–visible light spectra were recorded using a Varian Cary 100 Bio UV–visible spectrophotometer. The absorption maxima (λ_{\max}) in nm were reported together with the molar absorptivities (ϵ). HPLC quality tetrahydrofuran was used as the solvent for UV–vis measurements. High resolution mass spectra were acquired using a Thermo Scientific LTQ Orbitrap XL LC–MS mass spectrometer (electrospray ionization mode) in the Bioanalytical Mass Spectrometry Facility in the Mark Wainwright Analytical Centre at UNSW. Masses found for hydrogen adducts ($[\text{M}+\text{H}]^+$) and sodium adducts ($[\text{M}+\text{Na}]^+$) were reported with accuracy to four decimal places. Required masses were calculated using Xcalibur software installed on the spectrometer. Melting points were measured using a Mel-Temp melting point apparatus and are uncorrected. Both gravity column chromatography and flash column chromatography were performed using Grace Davisil LC60A 40–63 micron silica gel. Preparative thin layer chromatography was carried out using 3 mm \times 200 mm \times 200 mm glass plates coated with Merck Kieselgel 60 GF₂₅₄ silica gel. Reaction progress was monitored by thin-layer chromatography using Merck TLC Silica gel 60 F₂₅₄ aluminium sheets and detection by short and long wavelength ultraviolet light. Temperature quoted as 0 °C was achieved with a cooling bath of ice-water.

4.2. Synthetic chemistry details

4.2.1. Starting materials

The well-established methods developed in our group were utilized to synthesize 3-aryl-4,6-dimethoxyindoles **6a–b**,⁵⁶ 4,6-dimethoxy-3-methylindole **6c**,⁵⁶ 4,6-dimethoxy-2,3-dimethylindole **6d**⁵⁷ and 4,6-dimethoxy-3-phenylbenzofuran **11**⁵⁸ which were subsequently reacted with trichloroacetyl chloride and oxalyl chloride to afford respective 2-trichloroacetylindoles **8a–c**² and 7-trichloroacetylindoles **7a–b**,² indole-2-glyoxyloyl chlorides **10a–b**² and indole-7-glyoxyloyl chlorides **9a–b**.²

4,6-Dimethoxy-2,3-dimethylindole-7-glyoxyloyl chloride **9c** and 4,6-dimethoxy-3-phenylbenzofuran-2-glyoxyloyl chloride **12** were synthesized following the general procedure for the synthesis of glyoxyloyl chlorides² and purified by gravity column chromatography.

Indole-3-glyoxyloyl chloride **14** was prepared according to the literature procedure.⁵⁹

4.2.1.1. 4,6-Dimethoxy-2,3-dimethylindole-7-glyoxyloyl chloride (9c). Dark green solid (55%); mp 126–130 °C (decomp.); ¹H NMR (300 MHz, CDCl₃): δ 2.29 (s, 6H, Me), 3.94 (s, 3H, OMe), 4.00 (s, 3H, OMe), 6.06 (s, 1H, H5), 9.73 (br s, 1H, NH); ¹³C NMR (75 MHz, CDCl₃): δ 10.5, 11.2 (Me), 55.8, 56.8 (OMe), 86.6 (C5), 97.5 (C7), 108.2 (C3), 114.1 (C3a), 129.6 (C2), 136.8 (C7a), 161.4 (C6), 163.3 (C4), 165.2, 179.4 (C=O).

4.2.1.2. 4,6-Dimethoxy-3-phenylbenzofuran-2-glyoxyloyl chloride (12). Bright green solid (64%); mp 171–173 °C (decomp.); ¹H NMR (300 MHz, CDCl₃): δ 3.67 (s, 3H, OMe), 3.88 (s, 3H, OMe), 6.28 (d, J = 1.8 Hz, 1H, H5), 6.69 (d, J = 1.8 Hz, 1H, H7), 7.34–7.58 (m, 5H, ArH); ¹³C NMR (75 MHz, CDCl₃): δ 55.7, 56.1 (OMe), 87.9 (C5), 96.1 (C7), 112.1 (C3a), 127.6, 129.2 (ArCH), 130.3 (ArC), 130.4 (ArCH), 136.2 (C3), 143.5 (C2), 157.0 (C4), 158.8 (C7a), 164.3 (C6), 165.6, 174.7 (C=O).

4.2.2. General procedure for the synthesis of glyoxyloylamides **16j–m** and glyoxyloylhydrazides **16n–o**

To a solution of the respective glyoxyloyl chloride (1 mmol) in anhydrous diethyl ether (10–20 mL) was added excess aniline,

p-toluidine or phenylhydrazine and the reaction mixture stirred at room temperature for 1 h. The resulting precipitate was filtered out, washed with water and air-dried to afford the respective glyoxyloylamide or glyoxyloylhydrazide as a yellow solid in 27–41% yield.

4.2.2.1. 2-(3-(4-Bromophenyl)-4,6-dimethoxy-1H-indol-7-yl)-2-oxo-N-phenylacetamide (16j). Yellow solid (38%); mp 286–288 °C; ¹H NMR (300 MHz, DMSO-*d*₆): δ 3.82 (s, 3H, OMe), 3.94 (s, 3H, OMe), 6.50 (s, 1H, H5), 7.06–7.16 (m, 1H, ArH), 7.26 (d, J = 2.5 Hz, 1H, H2), 7.32–7.43 (m, 2H, ArH), 7.44–7.59 (m, 4H, ArH), 7.64–7.75 (m, 2H, ArH), 10.50 (s, 1H, NH), 11.62 (d, J = 2.1 Hz, 1H, NH); ¹³C NMR (75 MHz, DMSO-*d*₆): δ 55.8, 57.6 (OMe), 89.0 (C5), 101.2 (C7), 110.1 (C3), 116.4, 118.9 (ArC), 119.5, 123.5 (ArCH), 123.9 (C2), 128.9, 130.5, 131.1 (ArCH), 134.6, 137.1, 138.8, 161.0, 161.7 (ArC), 166.3, 188.0 (C=O); IR (KBr): ν_{\max} 3330 (NH), 1655 (C=O), 1585 (C=O), 1530, 1326, 1215, 1118 cm^{-1} ; UV–vis (THF): λ_{\max} 219 nm (ϵ 27,900 $\text{cm}^{-1} \text{M}^{-1}$), 238 (47,700), 331 (20,300); HRMS (+ESI): found m/z 479.0594 ($[\text{M}+\text{H}]^+$), $[\text{C}_{24}\text{H}_{19}\text{BrN}_2\text{O}_4\text{H}]^+$ requires m/z 479.0606 (monoisotopic mass).

4.2.2.2. 2-(3-(4-Chlorophenyl)-4,6-dimethoxy-1H-indol-7-yl)-2-oxo-N-phenylacetamide (16k). Yellow solid (28%); mp 286–289 °C; ¹H NMR (300 MHz, DMSO-*d*₆): δ 3.82 (s, 3H, OMe), 3.94 (s, 3H, OMe), 6.50 (s, 1H, H5), 7.06–7.16 (m, 1H, ArH), 7.26 (d, J = 2.5 Hz, 1H, H2), 7.32–7.45 (m, 4H, ArH), 7.50–7.61 (m, 2H, ArH), 7.65–7.74 (m, 2H, ArH), 10.50 (s, 1H, NH), 11.61 (d, J = 2.1 Hz, 1H, NH); ¹³C NMR (75 MHz, DMSO-*d*₆): δ 55.8, 57.6 (OMe), 89.0 (C5), 101.2 (C7), 110.2 (C3), 116.3 (ArC), 119.5, 123.5 (ArCH), 123.9 (C2), 127.6, 128.9 (ArCH), 130.4 (ArC), 130.7 (ArCH), 134.3, 137.1, 138.8, 161.0, 161.7 (ArC), 166.4, 188.0 (C=O); IR (KBr): ν_{\max} 3323 (NH), 1655 (C=O), 1585 (C=O), 1535, 1326, 1216, 1119, 1091 cm^{-1} ; UV–vis (THF): λ_{\max} 234 nm (ϵ 54,000 $\text{cm}^{-1} \text{M}^{-1}$), 252 (52,700), 337 (24,500); HRMS (+ESI): found m/z 435.1107 ($[\text{M}+\text{H}]^+$), $[\text{C}_{24}\text{H}_{19}\text{ClN}_2\text{O}_4\text{H}]^+$ requires m/z 435.1112 (monoisotopic mass).

4.2.2.3. 2-(3-(4-Bromophenyl)-4,6-dimethoxy-1H-indol-7-yl)-2-oxo-N-(*p*-tolyl)acetamide (16l). Yellow solid (41%); mp 275–277 °C. Found: C, 60.84; H, 4.29; N, 5.73; $\text{C}_{25}\text{H}_{21}\text{BrN}_2\text{O}_4$ requires: C, 60.86; H, 4.29; N, 5.68; ¹H NMR (300 MHz, DMSO-*d*₆): δ 2.29 (s, 3H, Me), 3.81 (s, 3H, OMe), 3.94 (s, 3H, OMe), 6.50 (s, 1H, H5), 7.13–7.22 (m, 2H, ArH), 7.26 (d, J = 2.5 Hz, 1H, H2), 7.43–7.66 (m, 6H, ArH), 10.40 (br s, 1H, NH), 11.61 (d, J = 2.2 Hz, 1H, NH); ¹³C NMR (75 MHz, DMSO-*d*₆): δ 20.5 (Me), 55.8, 57.6 (OMe), 89.0 (C5), 101.2 (C7), 110.1 (C3), 116.4, 118.9 (ArC), 119.5 (ArCH), 123.8 (C2), 129.3, 130.5, 131.1 (ArCH), 132.5, 134.6, 136.3, 137.2, 160.9, 161.7 (ArC), 166.2, 188.1 (C=O); IR (KBr): ν_{\max} 3332 (NH), 1652 (C=O), 1588 (C=O), 1536, 1325, 1215, 1094 cm^{-1} ; UV–vis (THF): λ_{\max} 203 nm (ϵ 67,000 $\text{cm}^{-1} \text{M}^{-1}$), 253 (36,200), 336 (16,000); HRMS (+ESI): found m/z 493.0756 ($[\text{M}+\text{H}]^+$), $[\text{C}_{25}\text{H}_{21}\text{BrN}_2\text{O}_4\text{H}]^+$ requires m/z 493.0763 (monoisotopic mass).

4.2.2.4. 2-(3-(4-Chlorophenyl)-4,6-dimethoxy-1H-indol-7-yl)-2-oxo-N-(*p*-tolyl)acetamide (16m). Yellow solid (27%); mp 275–277 °C. Found: C, 66.90; H, 4.67; N, 6.26; $\text{C}_{25}\text{H}_{21}\text{ClN}_2\text{O}_4$ requires: C, 66.89; H, 4.72; N, 6.24; ¹H NMR (300 MHz, DMSO-*d*₆): δ 2.29 (s, 3H, Me), 3.81 (s, 3H, OMe), 3.94 (s, 3H, OMe), 6.50 (s, 1H, H5), 7.17 (d, J = 8.3 Hz, 2H, ArH), 7.25 (d, J = 2.4 Hz, 1H, H2), 7.34–7.47 (m, 2H, ArH), 7.49–7.65 (m, 4H, ArH), 10.39 (s, 1H, NH), 11.60 (d, J = 1.5 Hz, 1H, NH); ¹³C NMR (75 MHz, DMSO-*d*₆): δ 20.5 (Me), 55.8, 57.6 (OMe), 89.0 (C5), 101.2 (C7), 110.1 (C3), 116.3 (ArC), 119.5 (ArCH), 123.8 (C2), 127.6, 129.2 (ArCH), 130.4 (ArC), 130.7

(ArCH), 132.5, 134.3, 136.3, 137.1, 160.9, 161.7 (ArC), 166.2, 188.1 (C=O); IR (KBr): ν_{\max} 3336 (NH), 1653 (C=O), 1585 (C=O), 1536, 1326, 1216, 1093 cm^{-1} ; UV-vis (THF): λ_{\max} 203 nm (ϵ 63,500 $\text{cm}^{-1} \text{M}^{-1}$), 253 (40,100), 336 (17,200); HRMS (+ESI): found m/z 449.1263 ([M+H]⁺), [C₂₅H₂₁ClN₂O₄H]⁺ requires m/z 449.1268 (monoisotopic mass).

4.2.2.5. 2-(3-(4-Bromophenyl)-4,6-dimethoxy-1H-indol-7-yl)-2-oxo-N-phenylacetohydrazide (16n). Yellow solid (31%); mp 248–250 °C; ¹H NMR (300 MHz, DMSO-*d*₆): δ 3.89 (s, 3H, OMe), 3.93 (s, 3H, OMe), 3.95 (s, 3H, OMe), 3.98 (s, 3H, OMe), 6.47 (s, 1H, H5), 6.51 (s, 1H, H5), 6.69–7.64 (m, 20H, H2, ArH), 7.74 (s, 1H, NH), 7.90 (d, J = 2.5 Hz, 1H, NH), 9.54 (s, 1H, NH), 10.13 (d, J = 2.5 Hz, 1H, NH), 11.50 (d, J = 2.0 Hz, 1H, NH), 11.58 (d, J = 2.0 Hz, 1H, NH); ¹³C NMR (75 MHz, DMSO-*d*₆): δ 55.8, 55.8, 57.0, 57.2 (OMe), 88.4, 88.8 (C5), 101.2, 101.4 (C7), 109.8, 110.0 (C3), 112.4, 113.5 (ArCH), 116.1, 116.3 (ArC), 118.6 (ArCH), 118.8, 118.9 (ArC), 119.6 (ArCH), 123.6, 123.7 (C2), 128.5, 128.7, 130.5, 130.5, 131.1, 131.1 (ArCH), 134.6, 134.7, 136.8, 137.1, 148.4, 149.3, 160.5, 160.9, 161.4, 161.8 (ArC), 167.7, 172.0, 188.9, 189.0 (C=O) (mixture of two rotamers in solid state due to hydrogen bonding); IR (KBr): ν_{\max} 3318 (NH), 3284, 1695 (C=O), 1578 (C=O), 1345, 1218, 1087 cm^{-1} ; UV-vis (THF): λ_{\max} 203 nm (ϵ 67,900 $\text{cm}^{-1} \text{M}^{-1}$), 232 (41,900), 337 (17,500); HRMS (+ESI): found m/z 494.0710 ([M+H]⁺), [C₂₄H₂₀BrN₃O₄H]⁺ requires m/z 494.0715 (monoisotopic mass).

4.2.2.6. 2-(3-(4-Chlorophenyl)-4,6-dimethoxy-1H-indol-7-yl)-2-oxo-N-phenylacetohydrazide (16o). Yellow solid (30%); mp 247–249 °C. Found: C, 63.89; H, 4.41; N, 9.38; C₂₄H₂₀ClN₃O₄ requires: C, 64.07; H, 4.48; N, 9.34; ¹H NMR (300 MHz, DMSO-*d*₆): δ 3.89 (s, 3H, OMe), 3.93 (s, 3H, OMe), 3.95 (s, 3H, OMe), 3.98 (s, 3H, OMe), 6.47 (s, 1H, H5), 6.51 (s, 1H, H5), 6.70–7.62 (m, 20H, H2, ArH), 7.73 (s, 1H, NH), 7.90 (d, J = 2.4 Hz, 1H, NH), 9.53 (s, 1H, NH), 10.13 (d, J = 2.4 Hz, 1H, NH), 11.49 (d, J = 2.2 Hz, 1H, NH), 11.57 (d, J = 2.2 Hz, 1H, NH); ¹³C NMR (75 MHz, DMSO-*d*₆): δ 55.8, 55.8, 57.0, 57.2 (OMe), 88.4, 88.8 (C5), 101.2, 101.4 (C7), 109.9, 110.0 (C3), 112.4, 113.5 (ArCH), 116.1, 116.3 (ArC), 118.6, 119.6 (ArCH), 123.6, 123.8 (C2), 127.5, 127.6, 128.5, 128.7 (ArCH), 130.3, 130.4 (ArC), 130.7, 130.7 (ArCH), 134.3, 134.3, 136.8, 137.1, 148.4, 149.3, 160.5, 160.9, 161.3, 161.8 (ArC), 167.7, 172.0, 188.9, 189.0 (C=O) (mixture of two rotamers in solid state due to hydrogen bonding); IR (KBr): ν_{\max} 3314 (NH), 3284, 1693 (C=O), 1581 (C=O), 1345, 1219, 1184, 1089 cm^{-1} ; UV-vis (THF): λ_{\max} 203 nm (ϵ 63,200 $\text{cm}^{-1} \text{M}^{-1}$), 231 (37,100), 253 (28,000), 337 (15,400); HRMS (+ESI): found m/z 450.1212 ([M+H]⁺), [C₂₄H₂₀ClN₃O₄H]⁺ requires m/z 450.1221 (monoisotopic mass).

4.2.3. General procedure for the synthesis of glyoxyloylamides 15a–e, 15l, 16a–i, 17a–d and 18a–d

To a solution or suspension of the respective glyoxyloyl chloride (0.3–2.3 mmol) in anhydrous diethyl ether (10–30 mL) was added excess amine (3–5 equiv) and the reaction mixture stirred at room temperature for 3–6 h. The resulting precipitate was filtered out, washed with diethyl ether (3 × 5 mL), 10% aqueous HCl solution (3 × 5 mL), water (3 × 5 mL) and air-dried to afford the respective glyoxyloylamide as a white, pink, yellow, orange or green solid in 30–88% yield. *Note 1:* additional recrystallization from isopropanol (5 mL) was performed for compounds **16a–b** and **16d**. *Note 2:* crude product **15d** was precipitated from the reaction mixture by addition of 10% aqueous HCl solution (30 mL), filtered out (after separation of the aqueous phase from the organic phase), washed with water (3 × 5 mL) and air-dried.

4.2.3.1. 1-(3-(4-Bromophenyl)-4,6-dimethoxy-1H-indol-2-yl)-2-(piperidin-1-yl)ethane-1,2-dione (15a). Bright yellow solid; mp 175–178 °C; ¹H NMR (300 MHz, DMSO-*d*₆): δ 1.17–1.41 (m, 4H, CH₂), 1.41–1.57 (m, 2H, CH₂), 2.90 (t, J = 4.8 Hz, 2H, CH₂), 3.04 (t, J = 4.8 Hz, 2H, CH₂), 3.56 (s, 3H, OMe), 3.80 (s, 3H, OMe), 6.15 (d, J = 1.8 Hz, H5), 6.51 (d, J = 1.8 Hz, H7), 7.18–7.31 (m, 2H, ArH), 7.46–7.58 (m, 2H, ArH), 11.93 (br s, 1H, NH); ¹³C NMR (75 MHz, DMSO-*d*₆): δ 23.6, 24.2, 25.1, 40.5, 46.1 (CH₂), 55.2, 55.4 (OMe), 86.2 (C5), 93.3 (C7), 112.5, 120.8, 125.4, 127.8 (ArC), 129.3 (ArCH), 132.3 (ArC), 133.0 (ArCH), 139.8, 156.2, 161.0 (ArC), 164.0, 182.8 (C=O); IR (KBr): ν_{\max} 3320 (NH), 2935, 2854, 1647 (C=O), 1600 (C=O), 1573 (C=O), 1521, 1482, 1297, 1251, 1220, 1163, 1127, 1074, 1003, 815, 771 cm^{-1} ; UV-vis (THF): λ_{\max} 210 nm (ϵ 63,800 $\text{cm}^{-1} \text{M}^{-1}$), 261 (27,800), 336 (23,500); HRMS (+ESI): found m/z 493.0729 ([M+Na]⁺), [C₂₃H₂₃BrN₂O₄Na]⁺ requires m/z 493.0733 (monoisotopic mass).

4.2.3.2. 1-(3-(4-Chlorophenyl)-4,6-dimethoxy-1H-indol-2-yl)-2-(piperidin-1-yl)ethane-1,2-dione (15b). Green-yellow solid (55%); mp 181–183 °C (decomp.); ¹H NMR (300 MHz, DMSO-*d*₆): δ 1.15–1.56 (m, 6H, CH₂), 2.89 (t, J = 4.8 Hz, 2H, CH₂), 3.04 (t, J = 4.8 Hz, 2H, CH₂), 3.55 (s, 3H, OMe), 3.80 (s, 3H, OMe), 6.14 (d, J = 1.9 Hz, 1H, H5), 6.50 (d, J = 1.9 Hz, 1H, H7), 7.23–7.33 (m, 2H, ArH), 7.33–7.43 (m, 2H, ArH), 11.92 (br s, 1H, NH); ¹³C NMR (75 MHz, DMSO-*d*₆): δ 23.6, 24.2, 25.1, 40.5, 46.1 (CH₂), 55.2, 55.4 (OMe), 86.2 (C7), 93.3 (C5), 112.6 (C3), 125.4 (C2), 126.4 (ArCH), 127.8, 131.9, 132.1 (ArC), 132.7 (ArCH), 139.8, 156.2, 160.9 (ArC), 164.0, 182.8 (C=O); IR (KBr): ν_{\max} 3322 (NH), 2935, 2855, 1650 (C=O), 1628 (C=O), 1601 (C=O), 1573 (C=O), 1522, 1484, 1298, 1251, 1220, 1164, 1127, 816, 771 cm^{-1} ; UV-vis (THF): λ_{\max} 213 nm (ϵ 25,800 $\text{cm}^{-1} \text{M}^{-1}$), 261 (18,600), 336 (18,600); HRMS (+ESI): found m/z 449.1241 ([M+Na]⁺), [C₂₃H₂₃ClN₂O₄Na]⁺ requires m/z 449.1239 (monoisotopic mass).

4.2.3.3. 1-(3-(4-Chlorophenyl)-4,6-dimethoxy-1H-indol-2-yl)-2-(morpholin-1-yl)ethane-1,2-dione (15c). Pale yellow solid (82%); mp 208–210 °C; ¹H NMR (300 MHz, DMSO-*d*₆): δ 2.93 (t, J = 4.4 Hz, 2H, CH₂), 3.11 (t, J = 4.4 Hz, 2H, CH₂), 3.28–3.48 (m, 4H, CH₂), 3.56 (s, 3H, OMe), 3.80 (s, 3H, OMe), 6.15 (d, J = 1.8 Hz, H5), 6.51 (d, J = 1.8 Hz, H7), 7.28–7.37 (m, 2H, ArH), 7.37–7.47 (m, 2H, ArH), 11.97 (s, 1H, NH); ¹³C NMR (75 MHz, DMSO-*d*₆): δ 40.2, 45.4 (CH₂), 55.2, 55.4 (OMe), 65.1, 65.4 (CH₂), 86.2 (C5), 93.4 (C7), 112.6, 125.7 (ArC), 126.5 (ArCH), 127.8, 131.9, 132.2 (ArC), 132.8 (ArCH), 140.0, 156.3, 161.1 (ArC), 164.4, 182.1 (C=O); IR (KBr): ν_{\max} 3304 (NH), 2967, 2933, 2862, 1644 (C=O), 1603 (C=O), 1577 (C=O), 1524, 1488, 1434, 1384, 1294, 1274, 1240, 1216, 1153, 1138, 1113, 1090, 1013, 818, 767 cm^{-1} ; UV-vis (THF): λ_{\max} 210 nm (ϵ 63,100 $\text{cm}^{-1} \text{M}^{-1}$), 261 (33,400), 339 (18,400); HRMS (+ESI): found m/z 451.1027 ([M+Na]⁺), [C₂₂H₂₁ClN₂O₅Na]⁺ requires m/z 451.1031 (monoisotopic mass).

4.2.3.4. 1-(3-(4-Bromophenyl)-4,6-dimethoxy-1H-indol-2-yl)-2-(pyrrolidin-1-yl)ethane-1,2-dione (15d). Grey-green solid (30%); mp 236–238 °C (decomp.); ¹H NMR (300 MHz, DMSO-*d*₆): δ 1.52–1.79 (m, 4H, CH₂), 2.75 (t, J = 6.8 Hz, 2H, CH₂), 3.15 (t, J = 6.8 Hz, 2H, CH₂), 3.56 (s, 3H, OMe), 3.80 (s, 3H, OMe), 6.15 (d, J = 1.9 Hz, 1H, H5), 6.50 (d, J = 1.9 Hz, 1H, H7), 7.15–7.29 (m, 2H, ArH), 7.42–7.57 (m, 2H, ArH), 11.94 (s, 1H, NH); ¹³C NMR (75 MHz, DMSO-*d*₆): δ 23.2, 25.2, 44.4, 45.6 (CH₂), 55.2, 55.4 (OMe), 86.2 (C7), 93.3 (C5), 112.4 (C3), 120.7 (ArC), 125.6 (C2), 127.4 (ArC), 129.4 (ArCH), 132.5 (ArC), 132.8 (ArCH), 139.9, 156.2, 161.0 (ArC), 163.9, 182.9 (C=O); IR (KBr): ν_{\max} 3329 (NH), 2958, 2882, 1642 (C=O), 1629 (C=O), 1615 (C=O), 1577 (C=O), 1521, 1483, 1452, 1268, 1207, 1154, 1137, 1011, 814, 698 cm^{-1} ; UV-vis (THF): λ_{\max} 213 nm (ϵ 48,600 $\text{cm}^{-1} \text{M}^{-1}$), 261 (20,700),

336 (18,800); HRMS (+ESI): found m/z 479.0578 ($[M+Na]^+$), $[C_{22}H_{21}BrN_2O_4Na]^+$ requires m/z 479.0577 (monoisotopic mass).

4.2.3.5. 1-(3-(4-Bromophenyl)-4,6-dimethoxy-1H-indol-2-yl)-2-(4-(pyridin-2-yl)piperazin-1-yl)ethane-1,2-dione (15e). White solid; mp 273–277 °C; 1H NMR (300 MHz, DMSO- d_6): δ 3.03 (br s, 2H, CH₂), 3.21 (t, J = 4.5 Hz, 2H, CH₂), 3.28–3.46 (m, 4H, CH₂), 3.56 (s, 3H, OMe), 3.81 (s, 3H, OMe), 6.15 (d, J = 1.9 Hz, H5), 6.51 (d, J = 1.9 Hz, H7), 6.64–6.72 (m, 1H, H5 pyridine), 6.78, 6.81 (2t, J = 0.75 Hz, 1H, H3 pyridine), 7.20–7.31 (m, 2H, ArH), 7.43–7.51 (m, 2H, ArH), 7.51–7.61 (m, 1H, H4 pyridine), 8.07–8.20 (m, 1H, H6 pyridine), 11.99 (s, 1H, NH); ^{13}C NMR (75 MHz, DMSO- d_6): δ 39.6, 43.5, 44.1, 44.6 (CH₂), 55.3, 55.4 (OMe), 86.2 (C5), 93.4 (C7), 107.3 (C3 pyridine), 112.5 (ArC), 113.5 (C5 pyridine), 120.9, 125.7, 127.8 (ArC), 129.4 (ArCH), 132.3 (ArC), 133.1 (ArCH), 137.7 (C4 pyridine), 140.0 (ArC), 147.6 (C6 pyridine), 156.3 (ArC), 158.4 (C2 pyridine), 161.1 (ArC), 164.5, 182.2 (C=O); IR (KBr): ν_{max} 3411 (NH), 3148 (NH), 3109 (NH), 3012, 2959, 2935, 2841, 1644 (C=O), 1614 (C=O), 1575 (C=O), 1488, 1435, 1240, 1204, 1157, 1134, 1008, 810, 770 cm^{-1} ; UV-vis (THF): λ_{max} 214 nm (ϵ 23,800 $cm^{-1} M^{-1}$), 254 (28,400), 337 (18,300); HRMS (+ESI): found m/z 571.0945 ($[M+Na]^+$), $[C_{27}H_{25}BrN_4O_4Na]^+$ requires m/z 571.0951 (monoisotopic mass).

4.2.3.6. Ethyl (2-(3-(4-chlorophenyl)-4,6-dimethoxy-1H-indol-2-yl)-2-oxoacetyl)glycinate (15l). Dark orange solid; mp 154–156 °C; 1H NMR (300 MHz, DMSO- d_6): δ 1.19 (t, J = 7.1 Hz, 3H, CH₂CH₃), 3.58 (s, 3H, OMe), 3.60 (d, J = 5.9 Hz, 2H, CH₂), 3.80 (s, 3H, OMe), 4.10 (q, J = 7.1 Hz, CH₂CH₃), 6.15 (d, J = 1.9 Hz, H5), 6.63 (d, J = 1.9 Hz, H7), 7.27–7.39 (m, 4H, ArH), 9.04 (t, J = 5.9 Hz, 1H, NH), 11.88 (s, 1H, NH); ^{13}C NMR (75 MHz, DMSO- d_6): δ 14.0 (CH₂CH₃), 40.2 (CH₂), 55.2, 55.3 (OMe), 60.6 (CH₂CH₃), 86.6 (C5), 93.3 (C7), 112.3, 126.2 (ArC), 126.5 (ArCH), 127.1, 131.6 (ArC), 132.5 (ArCH), 133.1, 139.7, 156.0, 160.8 (ArC), 164.9, 168.8, 179.3 (C=O); IR (KBr): ν_{max} 3386, 3318 (NH), 2970, 2938, 2839, 1747 (C=O), 1672 (C=O), 1617 (C=O), 1575 (C=O), 1510, 1479, 1384, 1311, 1259, 1207, 1157, 1131, 1089, 998, 815 cm^{-1} ; UV-vis (THF): λ_{max} 212 nm (ϵ 64,600 $cm^{-1} M^{-1}$), 262 (34,800), 359 (16,600); HRMS (+ESI): found m/z 467.0969 ($[M+Na]^+$), $[C_{22}H_{21}ClN_2O_6Na]^+$ requires m/z 467.0980 (monoisotopic mass).

4.2.3.7. 1-(3-(4-Bromophenyl)-4,6-dimethoxy-1H-indol-7-yl)-2-(piperidin-1-yl)ethane-1,2-dione (16a). Pale yellow solid (65%); mp 236–238 °C; 1H NMR (300 MHz, CDCl₃): δ 1.44–1.61 (m, 2H, CH₂), 1.61–1.74 (m, 4H, CH₂), 3.32 (t, J = 5.5 Hz, 2H, CH₂), 3.66 (br s, 2H, CH₂), 3.91 (s, 3H, OMe), 3.95 (s, 3H, OMe), 6.19 (s, 1H, H5), 7.09 (d, J = 2.3 Hz, 1H, H2), 7.34–7.52 (m, 4H, ArH), 10.75 (br s, 1H, NH); ^{13}C NMR (75 MHz, CDCl₃): δ 24.7, 25.4, 25.7, 41.8, 46.8 (CH₂), 55.6, 57.1 (OMe), 87.8 (C5), 102.0 (C7), 110.7 (C3), 118.0, 120.2 (ArC), 122.1 (C2), 130.8, 131.2 (ArCH), 134.4, 138.7, 161.7, 162.1 (ArC), 167.5, 190.4 (C=O); IR (KBr): ν_{max} 3389 (NH), 2930, 2855, 1637 (C=O), 1581 (C=O), 1560 (C=O), 1537, 1514, 1467, 1347, 1323, 1296, 1251, 1217, 1185, 1156, 1119, 1091, 1008, 798, 763 cm^{-1} ; UV-vis (THF): λ_{max} 211 nm (ϵ 13,600 $cm^{-1} M^{-1}$), 235 (15,500), 254 (20,900), 271 (16,900), 329 (15,600); HRMS (+ESI): found m/z 493.0730 ($[M+Na]^+$), $[C_{23}H_{23}BrN_2O_4Na]^+$ requires m/z 493.0733 (monoisotopic mass).

4.2.3.8. 1-(3-(4-Chlorophenyl)-4,6-dimethoxy-1H-indol-7-yl)-2-(piperidin-1-yl)ethane-1,2-dione (16b). Pale yellow solid (88%); mp 226–228 °C; 1H NMR (300 MHz, CDCl₃): δ 1.43–1.61 (m, 2H, CH₂), 1.61–1.80 (m, 4H, CH₂), 3.32 (t, J = 5.5 Hz, 2H, CH₂), 3.66 (br s, 2H, CH₂), 3.92 (s, 3H, OMe), 3.95 (s, 3H, OMe), 6.20 (s, 1H, H5), 7.09 (d, J = 2.3 Hz, 1H, H2), 7.28–7.36 (m, 2H, ArH), 7.42–7.52 (m, 2H, ArH), 10.74 (br s, 1H, NH); ^{13}C NMR (75 MHz, CDCl₃): δ 24.7, 25.4, 25.7, 41.8, 46.8 (CH₂), 55.6, 57.2 (OMe), 87.8

(C5), 102.1 (C7), 110.8 (C3), 118.0 (ArC), 122.1 (C2), 127.9, 130.8 (ArCH), 132.1, 134.0, 138.8, 161.8, 162.1 (ArC), 167.5, 190.4 (C=O); IR (KBr): ν_{max} 3395 (NH), 2936, 2857, 1625 (C=O), 1583 (C=O), 1561 (C=O), 1537, 1467, 1448, 1351, 1323, 1297, 1253, 1216, 1184, 1119, 1091, 1011, 798, 763 cm^{-1} ; UV-vis (THF): λ_{max} 211 nm (ϵ 30,300 $cm^{-1} M^{-1}$), 232 (28,400), 253 (34,000), 268 (24,800), 329 (21,300); HRMS (+ESI): found m/z 449.1238 ($[M+Na]^+$), $[C_{23}H_{23}ClN_2O_4Na]^+$ requires m/z 449.1239 (monoisotopic mass).

4.2.3.9. 1-(3-(4-Bromophenyl)-4,6-dimethoxy-1H-indol-7-yl)-2-(morpholin-1-yl)ethane-1,2-dione (16c). Pale yellow solid; mp 247–250 °C; 1H NMR (300 MHz, DMSO- d_6): δ 3.25 (t, J = 4.5 Hz, 2H, CH₂), 3.49–3.63 (m, 4H, CH₂), 3.69 (t, J = 4.5 Hz, 2H, CH₂), 3.95 (s, 3H, OMe), 3.96 (s, 3H, OMe), 6.50 (s, 1H, H5), 7.22 (d, J = 2.5 Hz, H2), 7.42–7.58 (m, 4H, ArH), 11.58 (d, J = 2.1 Hz, 1H, NH); ^{13}C NMR (75 MHz, DMSO- d_6): δ 40.6, 45.4 (CH₂), 55.9, 57.2 (OMe), 65.6, 65.8 (CH₂), 88.5 (C5), 101.3 (C7), 110.0, 116.4, 118.9 (ArC), 123.8 (C2), 130.5, 131.1 (ArCH), 134.6, 136.9, 161.2, 161.5 (ArC), 167.1, 188.7 (C=O); IR (KBr): ν_{max} 3292 (NH), 2956, 2922, 2853, 1633 (C=O), 1582 (C=O), 1557, 1530, 1348, 1275, 1214, 1178, 1112, 1024, 796, 763 cm^{-1} ; UV-vis (THF): λ_{max} 210 nm (ϵ 61,800 $cm^{-1} M^{-1}$), 255 (35,600), 331 (16,900); HRMS (+ESI): found m/z 495.0521 ($[M+Na]^+$), $[C_{22}H_{21}BrN_2O_5Na]^+$ requires m/z 495.0526 (monoisotopic mass).

4.2.3.10. 1-(3-(4-Chlorophenyl)-4,6-dimethoxy-1H-indol-7-yl)-2-(morpholin-1-yl)ethane-1,2-dione (16d). Pale yellow solid (76%); mp 239–241 °C; 1H NMR (300 MHz, CDCl₃): δ 3.39 (t, J = 4.5 Hz, 2H, CH₂), 3.67 (t, J = 4.5 Hz, 2H, CH₂), 3.70–3.76 (m, 2H, CH₂), 3.77–3.84 (m, 2H, CH₂), 3.92 (s, 3H, OMe), 3.98 (s, 3H, OMe), 6.20 (s, 1H, H5), 7.09 (d, J = 2.3 Hz, 1H, H2), 7.28–7.37 (m, 2H, ArH), 7.40–7.52 (m, 2H, ArH), 10.69 (br s, 1H, NH); ^{13}C NMR (75 MHz, CDCl₃): δ 41.3, 46.0 (CH₂), 55.7, 57.3 (OMe), 66.4, 66.7 (CH₂), 87.8 (C5), 102.0 (C7), 110.9 (C3), 118.2 (ArC), 122.2 (C2), 127.9, 130.8 (ArCH), 132.1, 133.8, 138.6, 162.1, 162.1 (ArC), 167.8, 189.5 (C=O); IR (KBr): ν_{max} 3377 (NH), 2974, 2906, 2852, 1635 (C=O), 1585 (C=O), 1559 (C=O), 1535, 1513, 1467, 1351, 1323, 1293, 1272, 1212, 1183, 1158, 1110, 1093, 1024, 973, 798, 764 cm^{-1} ; UV-vis (THF): λ_{max} 211 nm (ϵ 6,900 $cm^{-1} M^{-1}$), 235 (10,600), 254 (17,700), 270 (15,000), 332 (13,500); HRMS (+ESI): found m/z 451.1025 ($[M+Na]^+$), $[C_{22}H_{21}ClN_2O_5Na]^+$ requires m/z 451.1031 (monoisotopic mass).

4.2.3.11. 1-(3-(4-Chlorophenyl)-4,6-dimethoxy-1H-indol-7-yl)-2-(pyrrolidin-1-yl)ethane-1,2-dione (16e). Pale yellow solid (83%); mp decomp. >170 °C; 1H NMR (300 MHz, CDCl₃): δ 1.85–2.04 (m, 4H, CH₂), 3.38 (t, J = 6.5 Hz, 2H, CH₂), 3.62 (t, J = 6.5 Hz, 2H, CH₂), 3.91 (s, 3H, OMe), 3.94 (s, 3H, OMe), 6.18 (s, 1H, H5), 7.09 (d, J = 2.3 Hz, 1H, H2), 7.28–7.36 (m, 2H, ArH), 7.44–7.51 (m, 2H, ArH), 10.70 (br s, 1H, NH); ^{13}C NMR (75 MHz, CDCl₃): δ 24.5, 26.0, 45.1, 46.4 (CH₂), 55.6, 57.5 (OMe), 87.8 (C5), 101.5 (C7), 110.9 (C3), 118.1 (ArC), 122.1 (C2), 127.9, 130.8 (ArCH), 132.1, 133.9, 138.8, 161.8, 162.2 (ArC), 167.7, 190.2 (C=O); IR (KBr): ν_{max} 3385 (NH), 2968, 2878, 1626 (C=O), 1578 (C=O), 1556 (C=O), 1537, 1465, 1452, 1350, 1274, 1262, 1217, 1093, 979, 800 cm^{-1} ; UV-vis (THF): λ_{max} 211 nm (ϵ 32,100 $cm^{-1} M^{-1}$), 253 (24,200), 330 (14,800); HRMS (+ESI): found m/z 435.1091 ($[M+Na]^+$), $[C_{22}H_{21}ClN_2O_4Na]^+$ requires m/z 435.1082 (monoisotopic mass).

4.2.3.12. 1-(4-Benzylpiperazin-1-yl)-2-(3-(4-bromophenyl)-4,6-dimethoxy-1H-indol-7-yl)ethane-1,2-dione (16f). Pale yellow solid; mp 196–198 °C; 1H NMR (300 MHz, DMSO- d_6): δ 2.34 (t, J = 4.1 Hz, 2H, CH₂), 2.46 (t, J = 4.1 Hz, 2H, CH₂), 3.25 (t, J = 4.1 Hz, 2H, CH₂), 3.53 (s, 2H, CH₂ benzyl), 3.56 (t, J = 4.1 Hz, 2H, CH₂), 3.88 (s, 3H, OMe), 3.94 (s, 3H, OMe), 6.47 (s, 1H, H5), 7.22 (d, J = 2.6 Hz,

H2), 7.23–7.39 (m, 5H, ArH), 7.41–7.57 (m, 4H, ArH), 11.57 (d, $J = 2.3$ Hz, 1H, NH); ^{13}C NMR (75 MHz, DMSO- d_6): δ 40.2, 45.0, 51.7, 51.8 (CH₂), 55.9, 57.0 (OMe), 61.9 (CH₂ benzyl), 88.4 (C5), 101.3 (C7), 109.9, 116.3, 118.9 (ArC), 123.7 (C2), 127.1, 128.2, 129.0, 130.5, 131.1 (ArCH), 134.6, 136.9, 137.5, 161.1, 161.5 (ArC), 166.8, 188.9 (C=O); IR (KBr): ν_{max} 3407 (NH), 2938, 2811, 1636 (C=O), 1578 (C=O), 1558, 1349, 1217 cm^{-1} ; UV-vis (THF): λ_{max} 210 nm (ϵ 100,500 $\text{cm}^{-1} \text{M}^{-1}$), 253 (39,900), 318 (32,400); HRMS (+ESI): found m/z 584.1160 ([M+Na]⁺), [C₂₉H₂₈BrN₃O₄Na]⁺ requires m/z 584.1155 (monoisotopic mass).

4.2.3.13. 1-(4,6-Dimethoxy-2,3-dimethyl-1H-indol-7-yl)-2-(piperidin-1-yl)ethane-1,2-dione (16g). Yellow solid; mp 206–209 °C; ^1H NMR (300 MHz, DMSO- d_6): δ 1.36–1.50 (m, 2H, CH₂), 1.50–1.71 (m, 4H, CH₂), 2.24 (s, 3H, Me), 2.25 (s, 3H, Me), 3.17 (t, $J = 5.3$ Hz, 2H, CH₂), 3.50 (t, $J = 5.3$ Hz, 2H, CH₂), 3.86 (s, 3H, OMe), 3.98 (s, 3H, OMe), 6.34 (s, 1H, H5), 10.82 (s, 1H, NH); ^{13}C NMR (75 MHz, DMSO- d_6): δ 10.4, 10.7 (Me), 24.0, 24.9, 25.1, 40.7, 45.9 (CH₂), 55.9, 56.9 (OMe), 87.4 (C5), 101.3 (C7), 105.8 (C3), 113.1 (C3a), 130.0 (C2), 135.4 (C7a), 160.4 (C6), 160.6 (C4), 166.9, 189.2 (C=O); IR (KBr): ν_{max} 3532 (NH), 3356 (NH), 2922, 2849, 1637 (C=O), 1596 (C=O), 1561 (C=O), 1451, 1360, 1307, 1251, 1220, 1181, 1150, 1123, 990, 787 cm^{-1} ; UV-vis (THF): λ_{max} 210 nm (ϵ 35,200 $\text{cm}^{-1} \text{M}^{-1}$), 255 (27,000), 329 (11,600); HRMS (+ESI): found m/z 367.1619 ([M+Na]⁺), [C₁₉H₂₄N₂O₄Na]⁺ requires m/z 367.1628 (monoisotopic mass).

4.2.3.14. 1-(4,6-Dimethoxy-2,3-dimethyl-1H-indol-7-yl)-2-(morpholin-1-yl)ethane-1,2-dione (16h). Yellow solid; mp 277–280 °C (decomp.); ^1H NMR (300 MHz, DMSO- d_6): δ 2.23 (s, 3H, Me), 2.25 (s, 3H, Me), 3.21 (t, $J = 4.6$ Hz, 2H, CH₂), 3.48–3.61 (m, 4H, CH₂), 3.68 (t, $J = 4.6$ Hz, 2H, CH₂), 3.90 (s, 3H, OMe), 3.98 (s, 3H, OMe), 6.35 (s, 1H, H5), 10.83 (s, 1H, NH); ^{13}C NMR (75 MHz, DMSO- d_6): δ 10.4, 10.7 (Me), 40.5, 45.4 (CH₂), 55.9, 57.0 (OMe), 65.6, 65.8 (CH₂), 87.4 (C5), 101.2 (C7), 105.9 (C3), 113.2 (C3a), 130.1 (C2), 135.3 (C7a), 160.4 (C6), 160.9 (C4), 167.3, 188.5 (C=O); IR (KBr): ν_{max} 3363 (NH), 2915, 2853, 1652 (C=O), 1616, 1597 (C=O), 1561 (C=O), 1439, 1360, 1307, 1269, 1226, 1206, 1173, 1149, 1131, 1117, 1016, 988, 789 cm^{-1} ; UV-vis (THF): λ_{max} 210 nm (ϵ 29,200 $\text{cm}^{-1} \text{M}^{-1}$), 253 (25,600), 331 (12,600); HRMS (+ESI): found m/z 369.1414 ([M+Na]⁺), [C₁₈H₂₂N₂O₅Na]⁺ requires m/z 369.1421 (monoisotopic mass).

4.2.3.15. 1-(4,6-Dimethoxy-2,3-dimethyl-1H-indol-7-yl)-2-(4-pyridin-2-yl)piperazin-1-yl)ethane-1,2-dione (16i). Pale yellow solid; mp 264–266 °C (decomp.); ^1H NMR (300 MHz, DMSO- d_6): δ 2.24 (s, 3H, Me), 2.26 (s, 3H, Me), 3.27–3.37 (m, 2H, CH₂), 3.44–3.52 (m, 2H, CH₂), 3.56–3.71 (m, 4H, CH₂), 3.85 (s, 3H, OMe), 3.98 (s, 3H, OMe), 6.34 (s, 1H, H5), 6.64–6.72 (m, 1H, H5 pyridine), 6.83, 6.86 (2s, 1H, H3 pyridine), 7.50–7.63 (m, 1H, H4 pyridine), 8.07–8.21 (m, 1H, H6 pyridine), 10.86 (s, 1H, NH); ^{13}C NMR (75 MHz, DMSO- d_6): δ 10.4, 10.7 (Me), 39.9, 44.2, 44.3, 44.6 (CH₂), 55.9, 57.0 (OMe), 87.5 (C5), 101.3 (C7), 105.9 (C3), 107.4 (C3 pyridine), 113.2 (C3a), 113.5 (C5 pyridine), 130.1 (C2), 135.4 (C7a), 137.7 (C4 pyridine), 147.6 (C6 pyridine), 158.7 (C2 pyridine), 160.5 (C6), 160.9 (C4), 167.3, 188.7 (C=O); IR (KBr): ν_{max} 3415 (NH), 2924, 2852, 1650 (C=O), 1617, 1591 (C=O), 1557 (C=O), 1478, 1435, 1384, 1356, 1309, 1248, 1220, 1184, 1149, 1126, 1013, 984, 801, 776 cm^{-1} ; UV-vis (THF): λ_{max} 211 nm (ϵ 19,600 $\text{cm}^{-1} \text{M}^{-1}$), 252 (35,600), 329 (11,100); HRMS (+ESI): found m/z 445.1838 ([M+Na]⁺), [C₂₃H₂₆N₄O₄Na]⁺ requires m/z 445.1846 (monoisotopic mass).

4.2.3.16. 1-(1H-Indol-3-yl)-2-(piperidin-1-yl)ethane-1,2-dione (17a). White solid; mp 182–185 °C; ^1H NMR (300 MHz, DMSO- d_6): δ 1.33–1.51 (m, 2H, CH₂), 1.51–1.75 (m, 4H, CH₂), 3.22–3.32 (m, 2H, CH₂), 3.49–3.67 (m, 2H, CH₂), 7.19–7.38 (m, 2H, ArH), 7.50–7.58 (m, 1H, ArH), 8.05–8.25 (m, 2H, ArH), 12.28 (br s, 1H, NH); ^{13}C NMR (75 MHz, DMSO- d_6): δ 23.9, 25.0, 25.9, 41.2, 46.4 (CH₂), 112.6 (ArCH), 113.1 (ArC), 120.9, 122.5, 123.5 (ArCH), 124.8 (ArC), 136.8 (ArCH), 136.9 (ArC), 165.7, 186.8 (C=O); IR (KBr): ν_{max} 3152 (NH), 2920, 2857, 1612 (C=O), 1583 (C=O), 1519, 1498, 1462, 1444, 1270, 1244, 1161, 1128, 752, 738 cm^{-1} ; UV-vis (THF): λ_{max} 214 nm (ϵ 23,300 $\text{cm}^{-1} \text{M}^{-1}$), 245 (12,100), 264 (10,000), 302 (14,700); HRMS (+ESI): found m/z 257.1291 ([M+H]⁺), [C₁₅H₁₆N₂O₂H]⁺ requires m/z 257.1285 (monoisotopic mass).

4.2.3.17. 1-(1H-Indol-3-yl)-2-(morpholin-1-yl)ethane-1,2-dione (17b). Pale pink solid; mp 185–187 °C; ^1H NMR (300 MHz, DMSO- d_6): δ 3.24–3.45 (m, 2H, CH₂), 3.47–3.58 (m, 2H, CH₂), 3.58–3.67 (m, 2H, CH₂), 3.67–3.83 (m, 2H, CH₂), 7.15–7.42 (m, 2H, ArH), 7.45–7.66 (m, 1H, ArH), 8.06–8.18 (m, 1H, ArH), 8.21 (s, 1H, ArH), 12.34 (br s, 1H, NH); ^{13}C NMR (75 MHz, DMSO- d_6): δ 41.0, 46.0, 65.9, 66.2 (CH₂), 112.7 (ArCH), 113.1 (ArC), 120.9, 122.6, 123.6 (ArCH), 124.9, 137.0 (ArC), 137.3 (ArCH), 165.9, 186.0 (C=O); IR (KBr): ν_{max} 3157 (NH), 2977, 2925, 2860, 1613 (C=O), 1584 (C=O), 1519, 1443, 1242, 1157, 1113, 964, 783, 744 cm^{-1} ; UV-vis (THF): λ_{max} 212 nm (ϵ 26,000 $\text{cm}^{-1} \text{M}^{-1}$), 247 (13,000), 265 (11,100), 305 (15,700); HRMS (+ESI): found m/z 281.0904 ([M+Na]⁺), [C₁₄H₁₄N₂O₃Na]⁺ requires m/z 281.0897 (monoisotopic mass).

4.2.3.18. 1-(1H-Indol-3-yl)-2-(4-(pyridin-2-yl)piperazin-1-yl)ethane-1,2-dione (17c). White solid; mp 246–251 °C; ^1H NMR (300 MHz, DMSO- d_6): δ 3.39–3.58 (m, 4H, CH₂), 3.61–3.82 (m, 4H, CH₂), 6.63–6.73 (m, 1H, H5 pyridine), 6.82, 6.85 (2t, $J = 0.75$ Hz, 1H, H3 pyridine), 7.21–7.38 (m, 2H, ArH), 7.49–7.65 (m, 2H, H4 pyridine, ArH indole), 8.08–8.20 (m, 2H, H6 pyridine, ArH indole), 8.22 (s, 1H, ArH), 12.31 (br s, 1H, NH); ^{13}C NMR (75 MHz, DMSO- d_6): δ 40.3, 44.2, 44.9, 45.1 (CH₂), 107.4 (C3 pyridine), 112.7 (ArCH), 113.1 (ArC), 113.5 (C5 pyridine), 120.9, 122.6, 123.6 (ArCH), 124.9, 137.0 (ArC), 137.3 (C4 pyridine), 137.7 (ArCH), 147.6 (C6 pyridine), 158.6 (C2 pyridine), 165.9, 186.2 (C=O); IR (KBr): ν_{max} 3433 (NH), 3139 (NH), 3111 (NH), 2920, 1614 (C=O), 1591 (C=O), 1482, 1435, 1282, 1242, 1157, 957, 782, 742 cm^{-1} ; UV-vis (THF): λ_{max} 213 nm (ϵ 25,600 $\text{cm}^{-1} \text{M}^{-1}$), 250 (36,700), 305 (22,200); HRMS (+ESI): found m/z 335.1496 ([M+H]⁺), [C₁₉H₁₈N₄O₂H]⁺ requires m/z 335.1503 (monoisotopic mass).

4.2.3.19. 1-(4-Benzylpiperazin-1-yl)-2-(1H-Indol-3-yl)ethane-1,2-dione (17d). White solid; mp 175–178 °C; ^1H NMR (300 MHz, DMSO- d_6): δ 2.32 (t, $J = 4.9$ Hz, 2H, CH₂), 2.46 (t, $J = 4.9$ Hz, 2H, CH₂), 3.33 (t, $J = 4.9$ Hz, 2H, CH₂), 3.49 (s, 2H, CH₂ benzyl), 3.62 (t, $J = 4.9$ Hz, 2H, CH₂), 7.19–7.41 (m, 7H, ArH), 7.49–7.60 (m, 1H, ArH), 8.05–8.22 (m, 2H, ArH), 12.30 (br s, 1H, NH); ^{13}C NMR (75 MHz, DMSO- d_6): δ 40.6, 45.6, 52.0, 52.7 (CH₂), 61.8 (CH₂ benzyl), 112.7 (ArCH), 113.1 (ArC), 120.9, 122.5, 123.6 (ArCH), 124.8 (ArC), 127.1, 128.2, 128.9 (ArCH), 136.9 (ArC), 137.0 (ArCH), 137.7 (ArC), 165.8, 186.2 (C=O); IR (KBr): ν_{max} 3152 (NH), 3113 (NH), 3026, 2943, 2919, 2813, 2768, 1613 (C=O), 1584 (C=O), 1519, 1463, 1442, 1255, 1241, 1156, 1142, 998, 781, 775, 756, 746 cm^{-1} ; UV-vis (THF): λ_{max} 212 nm (ϵ 25,600 $\text{cm}^{-1} \text{M}^{-1}$), 246 (9,800), 265 (8,400), 304 (12,800); HRMS

(+ESI): found m/z 348.1710 ($[M+H]^+$), $[C_{21}H_{21}N_3O_2H]^+$ requires m/z 348.1707 (monoisotopic mass).

4.2.3.20. 1-(4,6-Dimethoxy-3-phenylbenzofuran-2-yl)-2-(piperidin-1-yl)ethane-1,2-dione (18a). Pale pink solid; mp 104–108 °C; 1H NMR (300 MHz, DMSO- d_6): δ 1.26–1.45 (m, 4H, CH₂), 1.45–1.64 (m, 2H, CH₂), 3.07 (t, J = 4.9 Hz, 2H, CH₂), 3.14 (t, J = 5.3 Hz, 2H, CH₂), 3.62 (s, 3H, OMe), 3.87 (s, 3H, OMe), 6.46 (d, J = 1.9 Hz, 1H, H5), 6.96 (d, J = 1.9 Hz, 1H, H7), 7.35–7.52 (m, 5H, ArH); ^{13}C NMR (75 MHz, DMSO- d_6): δ 23.7, 24.5, 25.3, 40.9, 46.2 (CH₂), 55.8, 56.1 (OMe), 88.2 (C5), 96.0 (C7), 111.1 (ArC), 127.0, 128.5 (ArCH), 129.6 (ArC), 130.3 (ArCH), 132.3, 143.6, 156.4, 157.3, 163.4 (ArC), 163.4, 180.8 (C=O); IR (KBr): ν_{max} 3464, 2939, 2858, 1640 (C=O), 1619 (C=O), 1594 (C=O), 1556, 1507, 1447, 1322, 1289, 1251, 1223, 1204, 1153, 1116, 1057, 813, 750 cm^{-1} ; UV-vis (THF): λ_{max} 210 nm (ϵ 26,100 $cm^{-1} M^{-1}$), 254 (18,600), 345 (22,100); HRMS (+ESI): found m/z 394.1654 ($[M+H]^+$), $[C_{23}H_{23}NO_5H]^+$ requires m/z 394.1649 (monoisotopic mass).

4.2.3.21. 1-(4,6-Dimethoxy-3-phenylbenzofuran-2-yl)-2-(morpholin-1-yl)ethane-1,2-dione (18b). Creamy white solid; mp 134–136 °C; 1H NMR (300 MHz, DMSO- d_6): δ 3.08 (t, J = 4.6 Hz, 2H, CH₂), 3.22 (t, J = 4.6 Hz, 2H, CH₂), 3.37–3.51 (m, 4H, CH₂), 3.63 (s, 3H, OMe), 3.87 (s, 3H, OMe), 6.46 (d, J = 1.9 Hz, 1H, H5), 6.97 (d, J = 1.9 Hz, 1H, H7), 7.34–7.59 (m, 5H, ArH); ^{13}C NMR (75 MHz, DMSO- d_6): δ 40.5, 45.5 (CH₂), 55.8, 56.1 (OMe), 65.3, 65.6 (CH₂), 88.2 (C5), 96.0 (C7), 111.1 (ArC), 127.1, 128.6 (ArCH), 129.6 (ArC), 130.4 (ArCH), 132.8, 143.6, 156.4, 157.4, 163.5 (ArC), 163.7, 180.1 (C=O); IR (KBr): ν_{max} 3444, 3120, 3059, 2957, 2913, 2856, 1642 (C=O), 1594 (C=O), 1552, 1509, 1464, 1443, 1322, 1272, 1232, 1204, 1152, 1115, 1008, 808 cm^{-1} ; UV-vis (THF): λ_{max} 210 nm (ϵ 29,500 $cm^{-1} M^{-1}$), 254 (19,300), 347 (22,300); HRMS (+ESI): found m/z 418.1258 ($[M+Na]^+$), $[C_{22}H_{21}NO_6Na]^+$ requires m/z 418.1261 (monoisotopic mass).

4.2.3.22. 1-(4,6-Dimethoxy-3-phenylbenzofuran-2-yl)-2-(4-pyridin-2-yl)piperazin-1-yl)ethane-1,2-dione (18c). Pale pink solid; mp 162–164 °C; 1H NMR (300 MHz, DMSO- d_6): δ 3.18 (t, J = 4.5 Hz, 2H, CH₂), 3.26–3.50 (m, 6H, CH₂), 3.62 (s, 3H, OMe), 3.87 (s, 3H, OMe), 6.46 (d, J = 1.8 Hz, 1H, H5), 6.63–6.72 (m, 1H, H5 pyridine), 6.78, 6.81 (2s, 1H, H3 pyridine), 6.97 (d, J = 1.8 Hz, 1H, H7), 7.31–7.50 (m, 5H, ArH), 7.50–7.60 (m, 1H, H4 pyridine), 8.04–8.20 (m, 1H, H6 pyridine); ^{13}C NMR (75 MHz, DMSO- d_6): δ 40.0, 43.7, 44.3, 44.7 (CH₂), 55.8, 56.1 (OMe), 88.2 (C5), 96.0 (C7), 107.3 (C3 pyridine), 111.1 (ArC), 113.5 (C5 pyridine), 127.1, 128.6 (ArCH), 129.6 (ArC), 130.4 (ArCH), 132.8 (ArC), 137.7 (C4 pyridine), 143.7 (ArC), 147.6 (C6 pyridine), 156.4, 157.4 (ArC), 158.4 (C2 pyridine), 163.5 (ArC), 163.7, 180.2 (C=O); IR (KBr): ν_{max} 3448, 3060, 3011, 2970, 2932, 2830, 1635 (C=O), 1590 (C=O), 1557, 1479, 1436, 1383, 1316, 1282, 1233, 1203, 1153, 1116, 981, 773, 753 cm^{-1} ; UV-vis (THF): λ_{max} 210 nm (ϵ 44,600 $cm^{-1} M^{-1}$), 253 (41,300), 346 (21,500); HRMS (+ESI): found m/z 494.1685 ($[M+Na]^+$), $[C_{27}H_{25}N_3O_5Na]^+$ requires m/z 494.1686 (monoisotopic mass).

4.2.3.23. 1-(4-Benzylpiperazin-1-yl)-2-(4,6-dimethoxy-3-phenylbenzofuran-2-yl)ethane-1,2-dione (18d). Pale yellow solid; mp 108–110 °C; 1H NMR (300 MHz, DMSO- d_6): δ 2.20 (t, J = 4.6 Hz, 2H, CH₂), 2.26 (t, J = 4.6 Hz, 2H, CH₂), 3.09 (t, J = 4.6 Hz, 2H, CH₂), 3.19 (t, J = 4.6 Hz, 2H, CH₂), 3.46 (s, 2H, CH₂ benzyl), 3.62 (s, 3H, OMe), 3.87 (s, 3H, OMe), 6.45 (d, J = 1.8 Hz, 1H, H5), 6.95 (d, J = 1.8 Hz, 1H, H7), 7.21–7.51 (m, 10H, ArH); ^{13}C NMR (75 MHz, DMSO- d_6): δ 40.2, 45.2, 51.2, 51.8 (CH₂), 55.8, 56.1 (OMe), 61.6 (CH₂ benzyl), 88.2 (C5), 96.0 (C7), 111.1 (ArC), 127.1, 127.1, 128.2, 128.6, 128.9 (ArCH), 129.5 (ArC), 130.3 (ArCH), 132.6, 137.5, 143.6,

156.4, 157.3, 163.4 (ArC), 163.4, 180.3 (C=O); IR (KBr): ν_{max} 3496, 2937, 2811, 1735, 1652 (C=O), 1613 (C=O), 1590 (C=O), 1551, 1504, 1445, 1366, 1321, 1221, 1202, 1152, 1117, 998, 745 cm^{-1} ; UV-vis (THF): λ_{max} 210 nm (ϵ 42,700 $cm^{-1} M^{-1}$), 254 (19,600), 346 (21,400); HRMS (+ESI): found m/z 507.1883 ($[M+Na]^+$), $[C_{29}H_{28}N_2O_5Na]^+$ requires m/z 507.1890 (monoisotopic mass).

4.2.4. General procedure for the synthesis of carboxamides 19 and 20a–c, and carboxhydrazides 20d–e

To a solution of the respective trichloroacetylindole (0.3–0.6 mmol) in anhydrous acetonitrile (20 mL) was added excess aniline, *p*-toluidine (25–95 equiv), phenylhydrazine (3 equiv) or morpholine (5 equiv) followed by triethylamine as a catalyst (5 drops) and the reaction mixture stirred at room temperature for 3–9 h (phenylhydrazine, morpholine) or heated at reflux overnight (aniline, *p*-toluidine). The solvent was evaporated under reduced pressure and the residue was treated with diethyl ether (10 mL). The resulting solid was filtered out and air-dried to afford the respective carboxamide or carboxyhydrazide as a white or yellow solid in 51–69% yield. *Note 1*: additional recrystallization from methanol was performed for compounds 20d–e. *Note 2*: product 19 was precipitated from the reaction mixture by addition of water (30 mL), filtered out, washed with water (3 × 5 mL) and air-dried.

4.2.4.1. (3-(4-Chlorophenyl)-4,6-dimethoxy-1H-indol-2-yl)(morpholino)methanone (19). Pale yellow solid (69%); mp decomp. >250 °C; 1H NMR (300 MHz, CDCl₃): δ 3.29 (br s, 8H, CH₂), 3.72 (s, 3H, OMe), 3.83 (s, 3H, OMe), 6.20 (d, J = 1.8 Hz, 1H, H5), 6.47 (d, J = 1.8 Hz, 1H, H7), 7.33–7.44 (m, 4H, ArH), 9.27 (br s, 1H, NH); ^{13}C NMR (75 MHz, CDCl₃): δ 55.2, 55.7 (OMe), 66.2 (CH₂), 86.5 (C7), 93.1 (C5), 110.8 (C3), 117.3 (ArC), 124.6 (C2), 128.0, 132.4 (ArCH), 133.1, 133.4, 138.0, 155.7, 159.2 (ArC), 164.3 (C=O); IR (KBr): ν_{max} 3276 (NH), 2959, 2930, 2849, 1625 (C=O), 1585 (C=O), 1536, 1457, 1270, 1230, 1208, 1151, 1134, 1115, 862, 823, 809, 750 cm^{-1} ; UV-vis (THF): λ_{max} 222 nm (ϵ 31,600 $cm^{-1} M^{-1}$), 252 (34,100), 305 (15,900); HRMS (+ESI): found m/z 423.1086 ($[M+Na]^+$), $[C_{21}H_{21}ClN_2O_4Na]^+$ requires m/z 423.1082 (monoisotopic mass).

4.2.4.2. 3-(4-Bromophenyl)-4,6-dimethoxy-N-phenyl-1H-indole-7-carboxamide (20a). White solid (60%); mp 226–228 °C; 1H NMR (300 MHz, CDCl₃): δ 3.90 (s, 3H, OMe), 4.13 (s, 3H, OMe), 6.31 (s, 1H, H5), 7.10–7.19 (m, 2H, H2, ArH), 7.34–7.43 (m, 2H, ArH), 7.43–7.53 (m, 4H, ArH), 7.63–7.72 (m, 2H, ArH), 10.05 (s, 1H, NH), 11.23 (br s, 1H, NH); ^{13}C NMR (75 MHz, CDCl₃): δ 55.4, 57.4 (OMe), 87.9 (C5), 98.3 (C7), 111.4 (C3), 117.0, 119.9 (ArC), 120.8 (ArCH), 122.4 (C2), 124.1, 129.1, 130.8, 131.2 (ArCH), 134.9, 138.6, 139.7, 156.7, 157.8 (ArC), 165.7 (C=O); IR (KBr): ν_{max} 3384 (NH), 1644 (C=O), 1591 (C=O), 1542, 1442, 1313, 1249, 975, 756 cm^{-1} ; UV-vis (THF): λ_{max} 246 nm (ϵ 35,400 $cm^{-1} M^{-1}$), 279 (22,500), 330 (23,900); HRMS (+ESI): found m/z 451.0649 ($[M+H]^+$), $[C_{23}H_{19}BrN_2O_3H]^+$ requires m/z 451.0657 (monoisotopic mass).

4.2.4.3. 3-(4-Bromophenyl)-4,6-dimethoxy-N-(*p*-tolyl)-1H-indole-7-carboxamide (20b). White solid (51%); mp 239–241 °C; 1H NMR (300 MHz, DMSO- d_6): δ 2.29 (s, 3H, Me), 3.91 (s, 3H, OMe), 4.12 (s, 3H, OMe), 6.56 (s, 1H, H5), 7.13–7.22 (m, 2H, ArH), 7.25 (d, J = 2.5 Hz, 1H, H2), 7.43–7.57 (m, 4H, ArH), 7.63–7.73 (m, 2H, ArH), 10.07 (s, 1H, NH), 11.50 (d, J = 1.7 Hz, 1H, NH); ^{13}C NMR (75 MHz, DMSO- d_6): δ 20.5 (Me), 55.5, 57.3 (OMe), 88.4 (C5), 98.2 (C7), 110.2 (C3), 115.4, 118.5 (ArC), 120.1 (ArCH), 123.6 (C2), 129.1, 130.4, 131.0 (ArCH), 132.3, 135.1, 136.3, 138.0, 156.1, 156.9 (ArC), 164.2 (C=O); IR (KBr): ν_{max} 3336 (NH), 1635 (C=O), 1587 (C=O), 1535, 1311, 1241, 978 cm^{-1} ; UV-vis (THF): λ_{max} 247 nm (ϵ 40,900 $cm^{-1} M^{-1}$), 238 (25,700), 331 (29,300);

HRMS (+ESI): found m/z 465.0808 ($[M+H]^+$), $[C_{24}H_{21}BrN_2O_3H]^+$ requires m/z 465.0814 (monoisotopic mass).

4.2.4.4. 3-(4-Chlorophenyl)-4,6-dimethoxy-*N*-(*p*-tolyl)-1*H*-indole-7-carboxamide (20c). White solid (56%); mp 234–236 °C; 1H NMR (300 MHz, DMSO- d_6): δ 2.29 (s, 3H, Me), 3.91 (s, 3H, OMe), 4.12 (s, 3H, OMe), 6.55 (s, 1H, H5), 7.13–7.21 (m, 2H, ArH), 7.24 (d, $J = 2.5$ Hz, 1H, H2), 7.34–7.43 (m, 2H, ArH), 7.49–7.59 (m, 2H, ArH), 7.63–7.73 (m, 2H, ArH), 10.07 (s, 1H, NH), 11.50 (d, $J = 1.6$ Hz, 1H, NH); ^{13}C NMR (75 MHz, DMSO- d_6): δ 20.5 (Me), 55.4, 57.3 (OMe), 88.4 (C5), 98.2 (C7), 110.3 (C3), 115.3 (ArC), 120.1 (ArCH), 123.6 (C2), 127.5, 129.1 (ArCH), 130.0 (ArC), 130.7 (ArCH), 132.3, 134.7, 136.3, 138.0, 156.1, 156.9 (ArC), 164.2 (C=O); IR (KBr): ν_{max} 3336 (NH), 1636 (C=O), 1592 (C=O), 1529, 1311, 1242, 978 cm^{-1} ; UV-vis (THF): λ_{max} 247 nm (ϵ 35,700 $cm^{-1} M^{-1}$), 282 (21,800), 330 (24,700); HRMS (+ESI): found m/z 421.1312 ($[M+H]^+$), $[C_{24}H_{21}ClN_2O_3H]^+$ requires m/z 421.1319 (monoisotopic mass).

4.2.4.5. 3-(4-Bromophenyl)-4,6-dimethoxy-*N*-phenyl-1*H*-indole-7-carbohydrazide (20d). Yellow solid (61%); mp 248–250 °C; 1H NMR (300 MHz, DMSO- d_6): δ 3.91 (s, 3H, OMe), 4.09 (s, 3H, OMe), 6.54 (s, 1H, H5), 6.67–6.76 (m, 1H, ArH), 6.78–6.88 (m, 2H, ArH), 7.10–7.23 (m, 3H, H2, ArH), 7.41–7.57 (m, 4H, ArH), 7.91 (d, $J = 3.1$ Hz, 1H, NH), 9.76 (d, $J = 3.1$ Hz, 1H, NH), 11.38 (d, $J = 2.1$ Hz, 1H, NH); ^{13}C NMR (75 MHz, DMSO- d_6): δ 55.4, 56.9 (OMe), 88.1 (C5), 96.5 (C7), 110.0 (C3), 112.4 (ArCH), 115.3 (ArC), 118.47 (ArCH), 118.48 (ArC), 123.4 (C2), 128.7, 130.4, 131.0 (ArCH), 135.1, 138.2, 149.8, 156.6, 156.9 (ArC), 166.5 (C=O); IR (KBr): ν_{max} 3346 (NH), 3315, 1641 (C=O), 1591 (C=O), 1540, 1343, 1270, 1218, 976 cm^{-1} ; UV-vis (THF): λ_{max} 202 nm (ϵ 56,300 $cm^{-1} M^{-1}$), 238 (42,400), 280 (22,100); HRMS (+ESI): found m/z 466.0759 ($[M+H]^+$), $[C_{23}H_{20}BrN_3O_3H]^+$ requires m/z 466.0766 (monoisotopic mass).

4.2.4.6. 3-(4-Chlorophenyl)-4,6-dimethoxy-*N*-phenyl-1*H*-indole-7-carbohydrazide (20e). White solid; mp 240–243 °C (decomp.); 1H NMR (300 MHz, DMSO- d_6): δ 3.91 (s, 3H, OMe), 4.09 (s, 3H, OMe), 6.54 (s, 1H, H5), 6.71 (t, $J = 7.2$ Hz, 1H, ArH), 6.78–6.91 (m, 2H, ArH), 7.07–7.28 (m, 3H, H2, ArH), 7.32–7.45 (m, 2H, ArH), 7.47–7.60 (m, 2H, ArH), 7.91 (d, $J = 2.9$ Hz, 1H, NH), 9.76 (d, $J = 2.9$ Hz, 1H, NH), 11.38 (d, $J = 1.6$ Hz, 1H, NH); ^{13}C NMR (75 MHz, DMSO- d_6): δ 55.4, 56.9 (OMe), 88.1 (C5), 96.5 (C7), 110.1 (C3), 112.4 (ArCH), 115.3 (ArC), 118.5 (ArCH), 123.4 (C2), 127.5, 128.7 (ArCH), 130.0 (ArC), 130.6 (ArCH), 134.7, 138.2, 149.9, 156.6, 156.9 (ArC), 166.5 (C=O); IR (KBr): ν_{max} 3359 (NH), 1645 (C=O), 1593 (C=O), 1536, 1345, 1215, 1102, 978, 754 cm^{-1} ; UV-vis (THF): λ_{max} 242 nm (ϵ 37,700 $cm^{-1} M^{-1}$), 284 (16,100), 295 (17,000); HRMS (+ESI): found m/z 422.1262 ($[M+H]^+$), $[C_{23}H_{20}ClN_3O_3H]^+$ requires m/z 422.1266 (monoisotopic mass).

4.2.5. General procedure for the synthesis of glyoxyloylamides 15f–k

To a solution of 4,6-dimethoxy-3-methylindole in anhydrous 1,2-dichloroethane (5 mL) prepared in a three-neck round-bottom flask and cooled to 0 °C was added oxalyl chloride (1.5 equiv) in one batch via syringe and the resulting mixture stirred under a nitrogen atmosphere for 30 min. The respective secondary heterocyclic amine (1.3–5.0 equiv) was added dropwise to a generated suspension of 4,6-dimethoxy-3-methylindole-2-glyoxyloyl chloride and the resulting reaction mixture heated at 60–70 °C under a nitrogen atmosphere for 3 h. After cooling to room temperature and quenching with water (15 mL) the organic phase was separated and the aqueous phase extracted with ethyl acetate (3 × 5 mL). Extracts were combined with the organic phase and dried over anhydrous sodium sulfate. The solution was mixed with silica gel and the solvents were removed in vacuo. Flash

chromatography (4.0–5.5 cm × 3.5 cm silica gel column filling, ethyl acetate/*n*-hexane 40%/60% (v/v) → 50%/50% (v/v) → 60%/40% (v/v)) afforded the respective glyoxyloylamides as yellow or brown solids in 10–54% yield.

Note: 1.3 equiv of *N*-benzylpiperazine and *N*-(pyridin-2-yl)piperazine, 2.0 equiv of *N*-methylpiperazine and pyrrolidine, and 5.0 equiv of morpholine and piperidine were used, respectively. Additional purification by preparative thin layer chromatography (ethyl acetate/*n*-hexane 35%/65% (v/v)) was performed for compound **15h** in order to obtain an analytically pure product.

4.2.5.1. 1-(4,6-Dimethoxy-3-methyl-1*H*-indol-2-yl)-2-(piperidin-1-yl)ethane-1,2-dione (15f). Pale yellow solid (42%); mp 215–218 °C; 1H NMR (300 MHz, CDCl₃): δ 1.50–1.62 (m, 2H, CH₂), 1.62–1.74 (m, 4H, CH₂), 2.67 (s, 3H, Me), 3.39 (t, $J = 5.4$ Hz, 2H, CH₂), 3.68 (t, $J = 5.4$ Hz, 2H, CH₂), 3.82 (s, 3H, OMe), 3.86 (s, 3H, OMe), 6.07 (d, $J = 1.8$ Hz, 1H, H5), 6.31 (d, $J = 1.8$ Hz, 1H, H7), 9.15 (br s, 1H, NH); ^{13}C NMR (75 MHz, CDCl₃): δ 12.0 (Me), 24.6, 25.4, 26.3, 42.3, 47.2 (CH₂), 55.4, 55.7 (OMe), 85.8 (C5), 93.0 (C7), 114.6 (C3a), 126.3 (C2), 128.0 (C3), 140.3 (C7a), 158.0 (C6), 162.1 (C4), 166.2, 181.5 (C=O); IR (KBr): ν_{max} 3443 (NH), 3243 (NH), 2936, 2857, 1630 (C=O), 1598 (C=O), 1576 (C=O), 1524, 1439, 1291, 1252, 1215, 1147, 802, 771 cm^{-1} ; UV-vis (THF): λ_{max} 212 nm (ϵ 43,500 $cm^{-1} M^{-1}$), 253 (20,900), 336 (30,900); HRMS (+ESI): found m/z 353.1468 ($[M+Na]^+$), $[C_{18}H_{22}N_2O_4Na]^+$ requires m/z 353.1472 (monoisotopic mass).

4.2.5.2. 1-(4,6-Dimethoxy-3-methyl-1*H*-indol-2-yl)-2-(morpholin-1-yl)ethane-1,2-dione (15g). Pale yellow solid (54%); mp 201–204 °C; 1H NMR (300 MHz, CDCl₃): δ 2.68 (s, 3H, Me), 3.41–3.58 (m, 2H, CH₂), 3.63–3.71 (m, 2H, CH₂), 3.72–3.80 (m, 4H, CH₂), 3.81 (s, 3H, OMe), 3.86 (s, 3H, OMe), 6.07 (d, $J = 1.8$ Hz, 1H, H5), 6.29 (d, $J = 1.8$ Hz, 1H, H7), 9.22 (br s, 1H, NH); ^{13}C NMR (75 MHz, CDCl₃): δ 12.1 (Me), 41.8, 46.5 (CH₂), 55.4, 55.7 (OMe), 66.6, 66.9 (CH₂), 85.8 (C5), 93.2 (C7), 114.6 (C3a), 127.0 (C2), 128.0 (C3), 140.5 (C7a), 158.1 (C6), 162.4 (C4), 166.2, 180.3 (C=O); IR (KBr): ν_{max} 3355 (NH), 2974, 2915, 2862, 1642 (C=O), 1579 (C=O), 1526, 1433, 1383, 1291, 1275, 1234, 1213, 1155, 1132, 1103, 987, 810, 752 cm^{-1} ; UV-vis (THF): λ_{max} 212 nm (ϵ 36,900 $cm^{-1} M^{-1}$), 254 (17,400), 337 (22,200); HRMS (+ESI): found m/z 355.1263 ($[M+Na]^+$), $[C_{17}H_{20}N_2O_5Na]^+$ requires m/z 355.1264 (monoisotopic mass).

4.2.5.3. 1-(4,6-Dimethoxy-3-methyl-1*H*-indol-2-yl)-2-(pyrrolidin-1-yl)ethane-1,2-dione (15h). Pale brown solid (10%); mp 159–161 °C; 1H NMR (300 MHz, CDCl₃): δ 1.94 (s, 4H, CH₂), 2.72 (s, 3H, Me), 3.44–3.74 (m, 4H, CH₂), 3.82 (s, 3H, OMe), 3.87 (s, 3H, OMe), 6.07 (s, 1H, H5), 6.29 (s, 1H, H7), 9.64 (br s, 1H, NH); ^{13}C NMR (75 MHz, CDCl₃): δ 12.3 (Me), 24.0, 26.4, 46.2, 47.6 (CH₂), 55.4, 55.7 (OMe), 85.8 (C5), 92.9 (C7), 114.5 (C3a), 127.3 (C2), 128.0 (C3), 139.9 (C7a), 158.0 (C6), 162.0 (C4), 165.2 (C=O), second C=O signal missing; IR (KBr): ν_{max} 3421 (NH), 3233 (NH), 2965, 2937, 2878, 2836, 1633 (C=O), 1596 (C=O), 1577 (C=O), 1524, 1420, 1384, 1326, 1271, 1220, 1154, 1131, 1079, 802 cm^{-1} ; UV-vis (THF): λ_{max} 212 nm (ϵ 31,300 $cm^{-1} M^{-1}$), 256 (15,300), 339 (17,100); HRMS (+ESI): found m/z 339.1310 ($[M+Na]^+$), $[C_{17}H_{20}N_2O_4Na]^+$ requires m/z 339.1315 (monoisotopic mass).

4.2.5.4. 1-(4,6-Dimethoxy-3-methyl-1*H*-indol-2-yl)-2-(4-(pyridin-2-yl)piperazin-1-yl)ethane-1,2-dione (15i). Brown solid (30%); mp 187–189 °C; 1H NMR (300 MHz, CDCl₃): δ 2.68 (s, 3H, Me), 3.41–3.74 (m, 6H, CH₂), 3.81, 3.85 (2s, 8H, CH₂, OMe), 6.06 (s, 1H, H5), 6.30 (s, 1H, H7), 6.52–6.83 (m, 2H, H5, H3 pyridine), 7.50 (t, $J = 6.7$ Hz, 1H, H4 pyridine), 8.18 (s, 1H, H6 pyridine), 9.27 (s, 1H, NH); ^{13}C NMR (75 MHz, CDCl₃): δ 12.1 (Me), 41.2,

45.0, 45.6, 45.8 (CH₂), 55.4, 55.7 (OMe), 85.8 (C5), 93.1 (C7), 107.5 (C3 pyridine), 114.3 (C5 pyridine), 114.6 (C3a), 126.9 (C2), 128.0 (C3), 137.9 (C4 pyridine), 140.5 (C7a), 148.1 (C6 pyridine), 158.1 (C2 pyridine), 159.0 (C6), 162.3 (C4), 166.4, 180.6 (C=O); IR (KBr): ν_{\max} 3415 (NH), 3308 (NH), 2934, 2838, 1639 (C=O), 1605 (C=O), 1588 (C=O), 1560 (C=O), 1523, 1476, 1434, 1381, 1296, 1231, 1213, 1159, 1129, 982, 776 cm⁻¹; UV-vis (THF): λ_{\max} 213 nm (ϵ 33,500 cm⁻¹ M⁻¹), 252 (31,400), 336 (20,100); HRMS (+ESI): found m/z 431.1689 ([M+Na]⁺), [C₂₂H₂₄N₄O₄Na]⁺ requires m/z 431.1690 (monoisotopic mass).

4.2.5.5. 1-(4-Benzylpiperazin-1-yl)-2-(4,6-dimethoxy-3-methyl-1H-indol-2-yl)ethane-1,2-dione (15j). Pale yellow solid (41%); mp 142–144 °C; ¹H NMR (300 MHz, CDCl₃): δ 2.44 (t, J = 4.0 Hz, 2H, CH₂), 2.53 (t, J = 4.0 Hz, 2H, CH₂), 2.67 (s, 3H, Me), 3.47 (t, J = 4.0 Hz, 2H, CH₂), 3.52 (s, 2H, CH₂ benzyl), 3.76 (t, J = 4.0 Hz, 2H, CH₂), 3.81 (s, 3H, OMe), 3.86 (s, 3H, OMe), 6.07 (s, 1H, H5), 6.30 (s, 1H, H7), 7.17–7.47 (m, 5H, ArH), 9.27 (s, 1H, NH); ¹³C NMR (75 MHz, CDCl₃): δ 12.0 (Me), 41.4, 46.1, 52.3, 53.0 (CH₂), 55.3, 55.6 (OMe), 62.9 (CH₂ benzyl), 85.9 (C5), 93.0 (C7), 114.5 (C3a), 126.6 (C2), 127.4 (ArCH phenyl), 128.0 (C3), 128.4 (ArCH phenyl), 129.2 (ArCH phenyl), 137.5 (ArC phenyl), 140.5 (C7a), 158.0 (C6), 162.1 (C4), 166.2, 181.0 (C=O); IR (KBr): ν_{\max} 3421 (NH), 3309 (NH), 2938, 2803, 1646 (C=O), 1608 (C=O), 1575 (C=O), 1522, 1437, 1241, 1215, 1152, 1130, 989, 811 cm⁻¹; UV-vis (THF): λ_{\max} 212 nm (ϵ 37,600 cm⁻¹ M⁻¹), 253 (14,100), 335 (18,100); HRMS (+ESI): found m/z 422.2073 ([M+H]⁺), [C₂₄H₂₇N₃O₄H]⁺ requires m/z 422.2074 (monoisotopic mass).

4.2.5.6. 1-(4,6-Dimethoxy-3-methyl-1H-indol-2-yl)-2-(4-methylpiperazin-1-yl)ethane-1,2-dione (15k). Bright yellow solid (39%); mp 192–194 °C; ¹H NMR (300 MHz, CDCl₃): δ 2.29 (s, 3H, N-Me), 2.37 (t, J = 4.4 Hz, 2H, CH₂), 2.48 (t, J = 4.4 Hz, 2H, CH₂), 2.65 (s, 3H, Me), 3.46 (t, J = 4.4 Hz, 2H, CH₂), 3.76 (t, J = 4.4 Hz, 2H, CH₂), 3.78 (s, 3H, OMe), 3.84 (s, 3H, OMe), 6.04 (s, 1H, H5), 6.29 (s, 1H, H7), 9.44 (br s, 1H, NH); ¹³C NMR (75 MHz, CDCl₃): δ 12.0 (Me), 41.3, 45.9 (CH₂), 46.1 (N-Me), 54.3, 54.9 (CH₂), 55.3, 55.6 (OMe), 85.8 (C5), 93.0 (C7), 114.5 (C3a), 126.7 (C2), 128.0 (C3), 140.6 (C7a), 158.0 (C6), 162.2 (C4), 166.2, 180.9 (C=O); IR (KBr): ν_{\max} 3343 (NH), 2970, 2938, 2857, 2800, 1641 (C=O), 1601 (C=O), 1578 (C=O), 1522, 1448, 1284, 1254, 1212, 1150, 990, 810, 771 cm⁻¹; UV-vis (THF): λ_{\max} 213 nm (ϵ 32,500 cm⁻¹ M⁻¹), 253 (15,600), 337 (21,100); HRMS (+ESI): found m/z 368.1576 ([M+Na]⁺), [C₁₈H₂₃N₃O₄Na]⁺ requires m/z 368.1581 (monoisotopic mass).

4.3. Biological assays

4.3.1. ELISA

Full-length σ^A was overproduced, purified²⁵ and diluted to 250 nM in phosphate buffered saline (PBS). 100 μ l of the solution was added into NUNC Maxisorp™ microtitre plate wells, followed by overnight incubation at 4 °C. The wells were washed three times with 300 μ l of PBS and blocked by incubating with 300 μ l of 1% (w/v) BSA in PBS at room temperature for 2 h. After blocking, plates were washed three times with wash buffer (PBS, 0.05% (v/v) Tween-20). 400 nM purified GST tagged RNAP β' subunit fragment²⁶ in 50 μ l PBS was mixed with 30 μ M compounds in 50 μ l PBS at 37 °C for 10 min, and then added to wells followed by incubation at room temperature for 1 h. Wells were washed three times with 300 μ l of PBS/Tween-20 wash buffer, 100 μ l of rabbit anti-GST primary antibody (1:2000 in PBS) was added to each well and the wells were incubated at room temperature for 1 h. Wells were washed three times with 300 μ l of PBS/Tween-20 wash buffer. HRP-conjugated goat-anti-rabbit secondary antibody (1:2000 in PBS) was added to each well and the wells were incubated at room temperature for 1 h. Interactions were detected by the

addition of 100 μ l TMB substrate system (3,3',5,5'-tetramethylbenzidine liquid substrate system for ELISA, Sigma–Aldrich) to each well. The plate was incubated with shaking at 600 rpm in a FLUOstar Optima plate reader (BMG Labtech) at room temperature for 6 min prior to measurement of the absorbance at 600 nm. Samples were tested in triplicate and the absorbance of each sample was compared to the control without exposure to compounds to calculate absolute inhibition percentages.

4.3.2. Growth inhibition assay

Compounds were dissolved at 50 mM in DMSO and then diluted to 200 μ M in 100 μ l of Luria–Bertani (LB) medium into individual wells in a 96-well plate. *E. coli* DH5 α or *B. subtilis* 168 cells were grown at 37 °C in 5 ml LB with shaking until the OD600 reached 0.6–0.7, and 5 μ l of the culture was added to each well. The plate was incubated in a FLUOstar Optima plate reader (BMG Labtech) at 37 °C shaking at 600 rpm. The OD600 of the culture was taken every 10 min over a 16 h period using LB as the blank. Samples were tested in triplicate and the growth pattern of each sample was compared to cells exposed to equal amounts of DMSO.

4.4. Prediction of molecular properties

Molecular properties of uncharged compounds were predicted using Discovery Studio (DS) software, version 4.0 (accel-rys.com). Pharmacophore mapping was also performed in DS using default parameters as described previously.⁴⁰

DS uses the following methods for these predictions: a Ghose–Crippen algorithm for $clogP$,⁶³ a method by Cheng and Merz for aqueous solubility⁶⁴ and a proprietary method for pK_a estimation based on reproducing the standard values for amino acids.⁶⁵

4.5. Crystallographic methods

A suitable single crystal of compound **16a** was selected under the polarizing microscope (Leica M165Z), mounted on a Micro-Mount (MiTeGen, USA) consisting of a thin polymer tip with a wicking aperture. The X-ray diffraction measurements were carried out on a Bruker kappa-II CCD diffractometer at 150 K by using μ S Incoatec Microfocus Source with Mo-K α radiation (λ = 0.710723 Å). The single crystal, mounted on the goniometer using cryo loops for intensity measurements, was coated with paraffin oil and then quickly transferred to the cold stream using an Oxford Cryo stream attachment.

During orientation matrix refinement, it became clear that these crystals show peculiar imperfection, as seen from the frames grabbed of reciprocal lattice views down a^* and b^* axis. The lattice rows along c^* show a slight modulation (upper figure, shown in Supplementary material) that results in non-exact superposition of lattice points while looking down b^* axis (lower figure, shown in Supplementary material). Several crystals were selected, but all exhibited the same behaviour.

Symmetry related absorption corrections using the program SADABS⁶⁶ were applied and the data corrected for Lorentz and polarisation effects using Bruker APEX2 software.⁶⁷ The structure was solved by Direct methods and the full-matrix least-square refinement was carried out using SHELXL.⁶⁸ The non-hydrogen atoms were refined anisotropically. The asymmetric unit contained four independent molecules in the asymmetric unit. After including all the non-H atoms and H-atoms, the final difference Fourier contained peaks $\sim 6 \text{ e } \text{Å}^{-3}$ near ($\sim 2 \text{ Å}$ away) from each of the four Br atoms. These could not be explained as any disordered (for example, water molecules) atoms. Also, the temperature factor of one of the carbon atoms C18B was non-positive definite during the refinement, which was restrained with the commands DELU

and SIMU. The two alerts at level A arising due to the above features (residual electron density peaks and anisotropy of C18B) should be attributed to the modulated lattice of these crystals. Although, this effect allowed us to proceed with the structure solution and refinement to the present level of accuracy.

5. Supplementary material

¹H NMR, ¹³C NMR and HRMS-ESI spectra and a table of molecular properties for all the compounds, additional software-generated figures related to the crystal structure of molecule **16a**, diagrams showing RNAP holoenzyme formation inhibition and bacterial growth inhibition curves for compounds **16c** and **18b**.

A cif file describing the crystal structure of compound **16a** (CCDC deposition number: 1022650).

Acknowledgments

This work was supported by a Project Grant from the National Health and Medical Research Council (NHMRC) Australia to N.K., P.L. and R.G. [NHMRC Grant APP1008014].

M.M. is thankful to UNSW Australia for a Tuition Fee Scholarship (TFS) and to N.K. for a Living Allowance Scholarship.

We are thankful to the Nuclear Magnetic Resonance Facility and the Bioanalytical Mass Spectrometry Facility in the Mark Wainwright Analytical Centre at UNSW Australia for an opportunity of using their measurement instruments.

Determination of IC₅₀ values for compounds **16c** and **18b** performed by Dr Samuel K. Kutty is greatly appreciated.

Supplementary data

Supplementary data associated with this article can be found, in the online version, at <http://dx.doi.org/10.1016/j.bmc.2015.02.037>. These data include MOL files and InChIKeys of the most important compounds described in this article.

References and notes

- Martinez, J. L. *Environ. Pollut.* **2009**, *157*, 2893.
- Mielczarek, M.; Devakaram, R. V.; Ma, C.; Yang, X.; Kandemir, H.; Purwono, B.; Black, D. StC.; Griffith, R.; Lewis, P. J.; Kumar, N. *Org. Biomol. Chem.* **2014**, *12*, 2882.
- French, G. L. *Int. J. Antimicrob. Agents* **2010**, *36*, S3.
- McAdam, A. J.; Hooper, D. C.; DeMaria, A.; Limbago, B. M.; O'Brien, T. F.; McCaughy, B. *Clin. Chem.* **2012**, *58*, 1182.
- Levy, S. B. *Sci. Am.* **1998**, *278*, 46.
- Neu, H. C. *Science* **1992**, *257*, 1064.
- Andersson, D. I.; Levin, B. R. *Curr. Opin. Microbiol.* **1999**, *2*, 489.
- Guillemot, D. *Curr. Opin. Microbiol.* **1999**, *2*, 494.
- Andersson, D. I. *Curr. Opin. Microbiol.* **2003**, *6*, 452.
- Alanis, A. J. *Arch. Med. Res.* **2005**, *36*, 697.
- Livermore, D. M. *Int. J. Antimicrob. Agents* **2007**, *29*, S1.
- Gould, I. M. *Int. J. Antimicrob. Agents* **2008**, *32*, S2.
- Gould, I. M. *Int. J. Antimicrob. Agents* **2009**, *34*, S2.
- Wilcox, M. H. *Int. J. Antimicrob. Agents* **2009**, *34*, S6.
- Livermore, D. M. *Lancet Infect. Dis.* **2005**, *5*, 450.
- Andersson, D. I.; Hughes, D. *Nat. Rev. Microbiol.* **2010**, *8*, 260.
- Barbosa, T. M.; Levy, S. B. *Drug Resist. Update.* **2000**, *3*, 303.
- Davies, J.; Davies, D. *Microbiol. Mol. Biol. Rev.* **2010**, *74*, 417.
- Levy, S. B. *J. Antimicrob. Chemother.* **2002**, *49*, 25.
- Levy, S. B. *Adv. Drug Delivery Rev.* **2005**, *57*, 1446.
- Levy, S. B. *Pediatr. Infect. Dis. J.* **2000**, *19*, S120.
- Yoshikawa, T. T. *J. Am. Geriatr. Soc.* **2002**, *50*, 226.
- Russell, A. D. *J. Appl. Microbiol.* **2002**, *92*, 1S.
- Witte, W. *J. Antimicrob. Chemother.* **1999**, *44*, 1.
- Levy, S. B. *N. Engl. J. Med.* **1998**, *338*, 1376.
- Hart, C. A. *Br. Med. J.* **1998**, *316*, 1255.
- Boucher, H. W.; Talbot, G. H.; Bradley, J. S.; Edwards, J. E.; Gilbert, D.; Rice, L. B.; Scheld, M.; Spellberg, B.; Bartlett, J. *Clin. Infect. Dis.* **2009**, *48*, 1.
- Peleg, A. Y.; Hooper, D. C. *N. Engl. J. Med.* **2010**, *362*, 1804.
- Chopra, I. *J. Antimicrob. Chemother.* **2013**, *68*, 496.
- Darst, S. A. *Trends Biochem. Sci.* **2004**, *29*, 159.
- Hinsberger, S.; Hüsecken, K.; Groh, M.; Negri, M.; Hauptenthal, J.; Hartmann, R. *W. J. Med. Chem.* **2013**, *56*, 8332.
- Villain-Guillot, P.; Bastide, L.; Gualtieri, M.; Leonetti, J.-P. *Drug Discovery Today* **2007**, *12*, 200.
- Villain-Guillot, P.; Gualtieri, M.; Bastide, L.; Leonetti, J.-P. *Antimicrob. Agents Chemother.* **2007**, *51*, 3117.
- André, E.; Bastide, L.; Michaux-Charachon, S.; Gouby, A.; Villain-Guillot, P.; Latouche, J.; Bouchet, A.; Gualtieri, M.; Leonetti, J.-P. *J. Antimicrob. Chemother.* **2006**, *57*, 245.
- Villain-Guillot, P.; Gualtieri, M.; Bastide, L.; Roquet, F.; Martinez, J.; Amblard, M.; Pugniere, M.; Leonetti, J.-P. *J. Med. Chem.* **2007**, *50*, 4195.
- Ho, M. X.; Hudson, B. P.; Das, K.; Arnold, E.; Ebright, R. H. *Curr. Opin. Struct. Biol.* **2009**, *19*, 715.
- Agarwal, A. K.; Johnson, A. P.; Fishwick, C. W. G. *Tetrahedron* **2008**, *64*, 10049.
- McClure, W. R. *J. Biol. Chem.* **1980**, *255*, 1610.
- Swanson, R. N.; Hardy, D. J.; Shipkowitz, N. L.; Hanson, C. W.; Ramer, N. C.; Fernandes, P. B.; Clement, J. J. *Antimicrob. Agents Chemother.* **1991**, *35*, 1108.
- Ma, C.; Yang, X.; Kandemir, H.; Mielczarek, M.; Johnston, E. B.; Griffith, R.; Kumar, N.; Lewis, P. J. *ACS Chem. Biol.* **2013**, *8*, 1972.
- Vassilyev, D. G.; Sekine, S.-I.; Laptchenko, O.; Lee, J.; Vassilyeva, M. N.; Borukhov, S.; Yokoyama, S. *Nature* **2002**, *417*, 712.
- Sharp, M. M.; Chan, C. L.; Lu, C. Z.; Marr, M. T.; Nechaev, S.; Merritt, E. W.; Severinov, K.; Roberts, J. W.; Gross, C. A. *Genes Dev.* **1999**, *13*, 3015.
- Patikoglou, G. A.; Westblade, L. F.; Campbell, E. A.; Lamour, V.; Lane, W. J.; Darst, S. A. *J. Mol. Biol.* **2007**, *372*, 649.
- Finn, R. D.; Orlova, E. V.; Gowen, B.; Buck, M.; van Heel, M. *EMBO J.* **2000**, *19*, 6833.
- Mekler, V.; Pavlova, O.; Severinov, K. *J. Biol. Chem.* **2011**, *286*, 270.
- Burgess, R. R.; Travers, A. A.; Dunn, J. J.; Bautz, E. K. F. *Nature* **1969**, *221*, 43.
- Callaci, S.; Heyduk, E.; Heyduk, T. *Mol. Cell* **1999**, *3*, 229.
- Helmann, J. D.; Chamberlin, M. J. *Annu. Rev. Biochem.* **1988**, *57*, 839.
- Arthur, T. M.; Anthony, L. C.; Burgess, R. R. *J. Biol. Chem.* **2000**, *275*, 23113.
- Malhotra, A.; Severinova, E.; Darst, S. A. *Cell* **1996**, *87*, 127.
- Lonetto, M.; Gribskov, M.; Gross, C. A. *J. Bacteriol.* **1992**, *174*, 3843.
- Johnston, E. B.; Lewis, P. J.; Griffith, R. *Protein Sci.* **2009**, *18*, 2287.
- Paterson, D. L. *Am. J. Med.* **2006**, *119*, S20.
- Perez, F.; Endimiani, A.; Hujer, K. M.; Bonomo, R. A. *Curr. Opin. Pharmacol.* **2007**, *7*, 459.
- Denton, M. *Int. J. Antimicrob. Agents* **2007**, *29*, S9.
- Pchalek, K.; Jones, A. W.; Wekking, M. M. T.; Black, D. StC. *Tetrahedron* **2005**, *61*, 77.
- Black, D. StC.; Kumar, N.; Wong, L. C. H. *Aust. J. Chem.* **1986**, *39*, 15.
- Black, D. StC.; Craig, D. C.; Kumar, N.; Rezaie, R. *Tetrahedron* **1999**, *55*, 4803.
- Guinchar, X.; Vallée, Y.; Denis, J.-N. *J. Org. Chem.* **2007**, *72*, 3972.
- Thompson, M. J.; Borsenberger, V.; Louth, J. C.; Judd, K. E.; Chen, B. *J. Med. Chem.* **2009**, *52*, 7503.
- Ortep-3 for Windows; Farrugia, L. J. *J. Appl. Crystallogr.* **2012**, *45*, 849.
- Krepski, L. R.; Hassner, A. J. *Org. Chem.* **1978**, *43*, 2879.
- Ghose, A. K.; Crippen, G. J. *Comput. Chem.* **1986**, *7*, 565.
- Cheng, A.; Merz, K., Jr. *J. Med. Chem.* **2003**, *46*, 3572.
- Creighton, T. E. *PROTEINS Structures and Molecular Properties*, 11nd Edition; W.H. Freeman: New York, 2002.
- Bruker, SADABS, Bruker AXS Inc., Madison, Wisconsin, USA, 2001.
- Bruker, APEX2 and SAINT, Bruker AXS Inc., Madison, Wisconsin, USA, 2007.
- Sheldrick, G. M. *Acta Crystallogr.* **2008**, *A64*, 112.